



Universität Hamburg
DER FORSCHUNG | DER LEHRE | DER BILDUNG



Impacts of bush encroachment on groundwater recharge – Evidence from 9 years of soil hydrological monitoring in a Namibian thornbush Savanna

Report

prepared for:

GIZ Office Namibia

Dr. Frank Gschwender
88, John Meinert Str
Windhoek, Namibia

prepared by:

Universität Hamburg

CEN Centrum für Erdsystemforschung und Nachhaltigkeit

Institut für Bodenkunde

Prof. Dr. Annette Eschenbach
Dr. Alexander Gröngröft
Allende-Platz 2
20146 Hamburg

Authors:

Dr. Alexander Gröngröft, Dr. Marleen de Blécourt, Nikolaus Classen, Lars Landschreiber & Prof. Dr. Annette Eschenbach

February 2018

Outline

1	INTRODUCTION AND OBJECTIVES	1
2	CURRENT KNOWLEDGE	2
2.1	Recharge rates.....	2
2.2	Methods to quantify recharge	4
2.3	Effects of bush encroachment on local soil water dynamics.....	5
3	DEFINITION OF THE SOIL WATER DOMAIN	8
4	CHARACTERISTICS OF THE STUDY AREA.....	10
4.1	Locality and land use	10
4.2	Soil properties	12
4.3	Vegetation	15
5	METHODS AND DATA OVERVIEW	19
5.1	Laboratory methods.....	19
5.2	Components of soil water monitoring stations	19
5.2.1	Climate	19
5.2.2	Soil water content and soil temperature.....	19
5.2.3	Soil water potential.....	19
5.3	Data Overview, processing and analysis	20
5.3.1	Data overview	20
5.3.2	Mean precipitation	21
5.3.3	Temperature corrections of soil water potentials.....	21
5.3.4	Balancing available soil water contents.....	22
5.3.5	Balancing flows to calculate deep percolation	22
6	RESULTS	24
6.1	Climate within the studied period	24
6.2	Rainwater Infiltration	26
6.3	Evapotranspiration.....	35
6.4	Deep percolation.....	45

7	DISCUSSION AND CONCLUSIONS	52
7.1	Reliability of the measured data	52
7.2	Impact of bush encroachment on the infiltration process	55
7.3	Impact of bush encroachment on the consumption of soil moisture	57
7.4	impact of bush encroachment on potential deep percolation	58
7.5	Conclusions, Open questions & outlook	59
8	REFERENCES	61

LIST OF FIGURES

Figure 1	Scheme of water fluxes of the savanna soil compartment	8
Figure 2	Location of the monitoring sites and farm boundary	12
Figure 3	Monitoring site EG	17
Figure 4	Monitoring site EL.....	17
Figure 5	Monitoring site ES.....	18
Figure 6	Mean distribution of rainfall	25
Figure 7	Linear correlation coefficients between daily rainfalls	26
Figure 8	Increase in soil water content following rain events for site ES – marked month of season.....	29
Figure 9	Increase in soil water content following rain events for site ES – marked initial SWC profile	29
Figure 10	Increase in soil water content following rain events for site ES – marked initial SWC topsoil.....	30
Figure 11	Increase in soil water content following rain events for site EL – marked month of season.....	31
Figure 12	Increase in soil water content following rain events for site EL – marked initial SWC profile	32
Figure 13	Increase in soil water content following rain events for site EL – marked initial SWC topsoil.....	32
Figure 14	Relation between initial SWC and δ SWC/rain for profile grass 1 (EG).....	33
Figure 15	Increase in soil water content following rain events for site EG – marked month of season.....	34
Figure 16	Increase in soil water content following rain events for site EG – marked initial SWC profile	34
Figure 17	Relation between SWC and loss of soil moisture (δ SWC) for site ES – profile canopy.....	36
Figure 18	Relation between SWP and loss of soil moisture (δ SWC) for site ES – profile canopy.....	37
Figure 19	Relation between SWP and loss of soil moisture (δ SWC) for site ES – profile intercanopy.....	37
Figure 20	Relation between SWC and loss of soil moisture (δ SWC) for site ES – profile intercanopy.....	38
Figure 21	Relation between SWC and loss of soil moisture (δ SWC) for site EL – profile canopy.....	39
Figure 22	Relation between SWP and loss of soil moisture (δ SWC) for site EL – profile canopy.....	39

Figure 23	Relation between SWC and loss of soil moisture (δ SWC) for site EL – profile intercanopy.....	40
Figure 24	Relation between SWP and loss of soil moisture (δ SWC) for site EL – profile intercanopy.....	40
Figure 25	Relation between SWP and loss of soil moisture (δ SWC) for site EG – both profiles.....	41
Figure 26	Relation between SWC and loss of soil moisture (δ SWC) for site EG –both profiles.....	42
Figure 27	Upper percentile (90) of the classified relation between δ SWC to SWP for all profiles.....	43
Figure 28	Median of the classified relation between δ SWC to SWP for all profiles.....	43
Figure 29	Measured hydraulic conductivity in relation to SWP (eight samples from site ES).....	45
Figure 30	Cumulative probability of SWP in 80 cm depth for the phase 10/2007 – 10/2016.....	47
Figure 31	Cumulative probability of SWP in 80 cm depth for the phase 4/2011 – 10/2016.....	47
Figure 32	Seasonal deep percolation in relation to rainfall.....	51
Figure 33	Example of the relation between SWP and SWC.....	53
Figure 34	Summary of the proportion of rainfall infiltration.....	56
Figure 35	Summary of daily water losses by evapotranspiration.....	57
Figure 36	Summary of potential deep percolation.....	58

List of tables

Table 1	Overview of the studied plots	11
Table 2	Properties of soil horizons: texture	13
Table 3	Properties of soil horizons: bulk density and porosity	14
Table 4	Properties of soil horizons: pH, EC, SOC, NT and CEC	15
Table 5	Results of plant analysis of 1000 m ² plots in 1998: Dominant species and coverage	16
Table 6	Density of woody vegetation within 1 ha (state 2/2010).....	16
Table 7	Overview of existing raw data	20
Table 8	Depth factors for balancing total soil water storage.....	22
Table 9	Precipitation for hydrological years measured on the farm (yellow: incomplete data; mean= sum of daily means of proper data)	24
Table 10	Registered most intensive rain events	25
Table 11	Rainwater infiltration at site ES – Summary of all events	29
Table 12	Rainwater infiltration at site EL – Summary of all events	31
Table 13	Rainwater infiltration at site EG – Summary of all events.....	34
Table 14	Pearson correlation coefficients (r) between daily evapotranspiration and the soil water storage and availability in different soil depth (highest coefficients for each profile in bold).....	44
Table 15	Frequency of moist subsoil water potentials (SWP).....	46
Table 16	Weighed probabilities of deep percolation.....	48
Table 17	Phases with moist subsoil and data availability for water balance approach.....	48
Table 18	Calculated deep percolation in phases with moist subsoil	50
Table 19	Comparison between soil hydrological properties measured in the laboratory and derived from field measurements of SWC and SWP	54

1 Introduction and objectives

The change in vegetation cover of African savannas with an increasing abundance of woody species is a widely observed phenomenon, which is addressed as 'bush encroachment'. The causes are discussed controversially (Van Auken 2000, de Klerk 2004, Briggs et al 2005, Ward 2005, Archer 2010, Eldridge et al 2011, O'Connor et al. 2014) and neither measures to avoid the bush thickening nor general accepted economic and sustainable strategies to reduce bush coverage are found until now. The encroachment of bushes has substantial economic impacts on the rangeland farmers, as the capacity of the grazing grounds for livestock is reducing. The number of livestock in bush-encroached rangelands has thus become much smaller compared to early times of rangeland management, for example commercial farms in Namibia from the late 1950s to about 30% (de Klerk 2004).

The increase in woody coverage and thus standing biomass is combined with shifts in carbon and nutrient stocks and flows. Different life strategies of woody plants compared to grasses are also addressed to the temporal and spatial dynamics of the uptake and consumption of water. Since the publications of Walter (1954) the difference in root distribution of trees and grasses is regarded as an indicator for varying water consumption strategies.

In general, in the semi-arid savannas the total amount of available water for plant growth is low and is restricted to the rainy season. The annual potential evapotranspiration typically exceeds the annual rainfall largely. Thus, the potential to recharge groundwater is generally very low and limited to years with extraordinary rainfall or to those parts of the landscape, where water can rapidly infiltrate in the deep underground or where water is concentrated by runoff.

The groundwater reserves have a high ecological and economical value, as the rural communities and the rangeland management depends on the available water from boreholes as drinking water for human and livestock.

If different patterns of water consumption for areas dominated by grasses and those with abundant bushes exist, then a change in patterns of groundwater recharge is likely. A decline in groundwater level has been observed in NW Namibia Christian & Associates (2010) and has been attributed to the observed bush-encroachment of the area. Also modelling approaches result in the same general conclusions (Chen et al. 2014), however, until now the model results could not be validated properly.

We observe the soil water dynamics of bush-encroached areas as well as de-bushed areas since 2007 with field monitoring techniques. The research aimed to understand the influence of different vegetation cover on the processes of soil water uptake and losses and thus to understand the water consumption strategies of the vegetation types. Although the groundwater recharge cannot be measured directly, the field measurements allow to quantify the number of days per year, when groundwater recharge is physically impossible and thus to

interpret the data with regard to the likelihood of groundwater recharge under varying vegetation. Additionally, modelling approaches are possible, which calculate all fluxes of the soil water dynamics and which can be validated by the field data.

Aiming at adding value to the yielded woody biomass, the de-bushing project of the GIZ tries to quantify the ecosystem services of different de-bushing measures. Here, the differences in groundwater recharge between encroached and de-bushed areas play an important role in the choice of action alternatives. However, the quantification of the ESS 'groundwater recharge' is confronted with a high uncertainty regarding the scientific knowledge of the ecological effects.

To potentially reduce the knowledge gaps, this report has the following objectives:

- i. To summarize the scientific knowledge about the patterns and processes involved with the groundwater recharge of semi-arid savannas (chapter 2),
- ii. To present background information on the studied sites (chapter 4),
- iii. To document the applied methods (chapter 5),
- iv. To show measured data with a special focus on the involved processes 'rain water infiltration', 'evapotranspiration' and 'deep percolation' (chapter 6),
- v. To discuss the results with regard to spatial and temporal extrapolation and open questions (chapter 7).

2 Current knowledge

Knowledge about groundwater recharge is crucial for all water use and management options. Although of the high relevance, Kinzelbach et al. (2002) characterized the quantification problem as: *"The rate of recharge is the single most important factor in the analysis and management of groundwater resources in arid and semi-arid regions. At the same time, it is also the most difficult quantity to determine."* The following chapters try to report on the current knowledge with regard to the groundwater recharge rate in drylands, the methodology for the quantification and the effects of encroaching trees on soil water dynamics.

2.1 RECHARGE RATES

A global synthesis of rates and controlling processes of the groundwater recharge in arid and semiarid regions have been prepared by Scanlon et al (2006). They found, that for large areas the range of mean recharge rate is 0.2 to 35 mm a⁻¹ which represents 0.1 to 5 % of the long-term mean annual precipitation. In areas with < 200 mm annual precipitation recharge rates are found negligible. There were no studies from Namibia available, nearest results come from Botswana (e.g. deVries et al 2000) and South Africa (Butler & Verhagen 2001).

Recharge rates in (semi-) arid environments are controlled by numerous factors of which climate, land-use and soil conditions are regarded as dominating.

The annual climate variability e. g. the effects of El Niño may result in up to threefold higher recharge rates.

Groundwater recharge is related to land use (LU). For Niger, a study (see Scanlon et al. 2006) found, that the recharge rate for natural savanna ecosystems was between 1- 5 mm a⁻¹, which was increased by cultivation by one order of magnitude. For cultivated areas, the soil crusting and increased surface runoff may enhance the recharge to local ponds, where enlarged groundwater recharge is possible. Although in the Sahel zone severe droughts were observed in the 1970s and 1980s, the groundwater level increased due to LU change. In Australia, the change of the natural deep-rooting eucalyptus vegetation to shallow-rooted crops and grasslands have increased recharge rates significantly. For all 14 studies assessed by Scanlon et al. (2006) on clearing effects, a significant increase in mean annual recharge has been found.

Additionally, to climate and land use, also the soil properties and the underlying bedrock modify groundwater recharge. For the Sahel, recharge rates were highest (~ 20 mm a⁻¹) at thick quaternary sands and decreased to low values (~ 1 mm a⁻¹) at finer textured soils (Scanlon 2006). For the studies in the central Kalahari basin, extremely low recharge rates (~ 1 mm a⁻¹) have been found under precipitation regime of 350-450 mm a⁻¹ (deVries 2000). In the eastern part of the basin the groundwater recharge is likely to be influenced by preferential flows below local pans. Also for the southern part of the Kalahari, Butler & Verhagen (2001) had evidence for preferential flows, as the recharge rates calculated from tritium profiles were significantly larger (~ 13 mm a⁻¹) than those calculated from chloride profiles (1.8-5 mm a⁻¹) of the unsaturated zone. The detailed studies in the mountainous drylands of Southwest USA have resulted in conceptual and numerical models for the regional groundwater recharge. The local recharge rates are highly variable, with highest rates (> 500 mm a⁻¹) observed in active channel positions in areas with thin soil layers and high bedrock permeability. In contrast, in areas with low permeable granites simulated recharge rate were much lower (< 2 mm a⁻¹).

Giving an overview of the groundwater situation in Namibia, Christelis et al. (2001) mentioned the insufficient knowledge about groundwater recharge even in areas with intensive water abstraction due to the short time of monitoring. However, a strong correlation between rainfall and recharge has become evident based on comparisons of rainfall records with groundwater levels.

For the Namibian Agricultural Union Christian & Associates (2010) prepared a desk-top study on *“The Effect of Bush Encroachment on Groundwater Resources in Namibia”*. The authors collected data i) on the size and specific water consumption of encroacher bushes and grasses, and ii) on the biomass production and the water-use efficiency. Based on these data, they calculated the amount of water consumptions by 2400 encroacher bushes per hectare with three methods (1: the annual woody biomass production * water needed for production; 2: number of normalized trees * specific water consumption per 8 hours; 3: total canopy area *

specific water consumption), all coming to the result that the shrubs consume about 60 % of the annual precipitation of 400 mm. For a vegetation composition with a favorable tree component they calculated a reduced transpiration of about 120 mm. For one example (the Platveld aquifer study) and one strong rain event evidence was presented that on a de-bushed area of a farm the groundwater level (data of 1 monitoring well) rose significantly stronger than for the bush encroached areas around (data of 4 monitoring wells). Furthermore, calculations were presented that by reducing the bush density to the original density some 50 to 80 years ago, an increase of groundwater recharge up to 4 % of the mean annual precipitation can be expected.

2.2 METHODS TO QUANTIFY RECHARGE

The methods to quantify groundwater recharge in drylands have been assessed and reported by Kinzelbach et al. (2002) for the UNEP. They found a brought array of methods applied, however, due to specific conditions of the drylands there is no single method which can generally be advised. Methods are categorized in

- Direct measurements of groundwater recharge
- Water balance methods (including hydrograph methods)
- Darcyan methods
- Tracer methods

of which the methods applied in our study are listed in the first category in combination with the second. The advantages of this methodological approach are given with the direct measure of soil water content which can be used for budgeting e.g. with water balance methods. Disadvantages are the restricted spatial information (point data) and that more information is needed to get a complete water balance. Moreover, the interpretation of soil profiles may not be accurate, if there is disturbance by lateral flow, which makes the assumption of 1D vertical flux doubtful. Finally, the accuracy for estimation of regional values is not quantifiable due to unknown spatial variability.

The quantification of deep percolation with soil water balance models is an appropriate method to combine local climate, soil and vegetation knowledge with hydrological system understanding. Bennett et al. (2013) used the SWAP model to estimate the uncertainty of deep percolation for an area in the northern part of SW Australia with different land-use types for 26 years. They found, that rainfall variation explains variability of deep percolation to about 55 %, the second largest factor was found in land-use with about 37 % explained uncertainty. Variability in soil hydraulic properties contributed only with about 8 % to the uncertainty of deep percolation. The authors conclude, that knowledge about rainfall patterns in space and time is crucial for a robust prediction of deep percolation and that long-term data are needed to capture the episodic rainfall distributions.

2.3 EFFECTS OF BUSH ENCROACHMENT ON LOCAL SOIL WATER DYNAMICS

In general, savannas are characterized by a mixture of a herbaceous layer with interspersed tree in a subtropical location with a distinct seasonal rainfall distribution (Scholes & Walker 1993). The evolution of these ecosystems is strongly correlated to the evolution of large grazing herbivores (McCarthy & Rudidge 2005) and thus the impact of ungulates is regarded a necessary factor for the stability of savannas. There has been a long debate about the causes of increasing density of woody vegetation in African rangelands (e.g. Van Auken 2000, Briggs et al 2005, Ward 2005, Eldridge et al 2011, Archer 2010, O'Connor et al. 2014). One explanation is linked to the competition-driven model of the coexistence of trees and grasses in savannas: Grasses and trees compete about the soil moisture with separated root systems. In the upper soil layer grasses and trees are in competition, but trees have advantages, if the deeper layer becomes moistened, where only tree roots are existing. The proportion of moisture in the deep layer is suggested to increase if a) grasses are heavily grazed for years or if b) soils are more sandy. This model explains, that sandy areas tend to be more encroached than areas with fine-grained soils. This model is thought to be relevant especially under more dry conditions, as in moist savannas the upper soil layer is generally supporting both trees and grasses. A second explanation for tree-grass-interaction is the demographic bottleneck model, which regards the influence of climate variability and disturbance on the growth and mortality of trees as the main factor for tree and grass coexistence. Here, e.g. the fire frequency controls the likelihood of tree recruitment, as seedlings are killed by the fire.

The mechanisms of competition and facilitation of grasses and trees in savannas have been reviewed by Scholes & Archer (1997) including the interaction to soil water dynamics. Processes like stemflow, shading, interception from the tree crown and hydraulic lift, are likely to shape the water dynamics in the canopy and inter-canopy area. Stemflow water may be deep percolating, facilitated by low bulk densities and root channels, a process likely to favor deep-rooting trees. The overview given by Scholes & Archer (1997) was based on a number of scientific papers, whose relevance for the Namibian Savannas is questionable due to different climatic and soil conditions. As a robust finding for the role of trees on the water balance, often Joffre & Rambal (1993) is cited. These authors have measured the influence of evergreen oak trees in a Mediterranean setting in southern Spain for three rainy seasons. They showed that under a dominating winter rainfall regime, the annual evapotranspiration of the tree canopy patch was significantly larger (on average 590 mm) compared to the grassy intercanopy patch (400 mm). Consequently, the calculated deep percolation was negligible below the trees as far as precipitation was below 500 mm, whereas in the intercanopy area from 500 mm precipitation 200 mm deep percolation could be expected.

Huxman et al. (2005) studied the impacts of bush encroachment on eco-hydrological processes on the landscape scale based on findings in the literature. They developed two conceptual models on the role trees on run-off generation and transpiration and drew the conclusions that woody plants have the potential to affect water budgets. Due to shifts in leaf area, volume of root systems and duration of physiological activities they expect changes in the

ratio of transpiration to total evapotranspiration which are more pronounced in semiarid landscapes than in arid or sub-humid ecosystems. From a general overview of the relation of evapotranspiration (ET) to total precipitation (P) given by Zhang et al (2001), it can be seen, that the ratio ET/P for woody vegetation exceeds the ratio for non-woody vegetation significantly. The conclusion of this ratio is, that *“in arid zones (defined with $P < 350$ mm) all precipitation is essentially lost to the atmosphere, and differences (in ET/P) between woody and nonwoody systems are very small. In semiarid zones ($350 \text{ mm} < P < 800 \text{ mm}$), the relative effect changes dramatically as a function of P.”*

Studying rangelands and bush encroachment, Archer (2010) found *“relatively little quantitative information regarding how increases in woody plant abundance may have changed the hydrological cycle...”*. Based on grey literature he summarizes, that the *“effects of shrub removal on stream flow vary, depending on the traits of the woody plants (their canopy and rooting architecture), climate (e.g. rainfall amount, seasonality, event sizes and intensities), soil type (deep vs. shallow; sandy vs. clayey) and geomorphology (Thurow & Hester 1997; Huxman et al. 2005; Wilcox et al. 2006). There may be little potential for increasing stream flow where annual precipitation (PPT) is less than 500 mm (Wilcox 2002; Wilcox et al. 2005). Thus, broad generalizations regarding shrub control effect on water yield should be viewed with suspicion.”*

The emerging issue of studying rangeland eco-hydrology has been highlighted by Wilcox & Thurow (2006). They reported clear evidence of the effect of trees on enlarged evapotranspiration compared to grasslands for humid, montane and Mediterranean ecosystems. However, for semi-arid rangelands the relation of de-bushing to increased water yields has not been demonstrated properly on the landscape scale, which is relevant for water harvesting. Wilcox & Thurow found that existing field studies on changes in the water budgets *“tend to be site-specific, tenuous, and difficult to measure accurately (Huxman et al. 2005). One problem is that the anticipated reductions in ET from tree and shrub removal can be offset by increases in transpiration from the herbaceous plants and by evaporation from newly exposed soil.”* As a consequence of the recent knowledge, they propose to increase *“research into the ecohydrologic implications of changing woody plant cover will realize the greatest benefits by focusing on 1) improving our understanding of pathways and processes of streamflow generation; 2) accurately identifying “hydrologically sensitive” areas on the landscape—those likely to have the potential for significant increases in water yield from shrub control; and 3) conducting more research, aided by stable isotope technologies, to understand where the woody plants are accessing water throughout the soil profile and how this water is hydrologically connected to the rest of the landscape.”*

Wiegand et al. (2005) conducted a study on the patchiness of the vegetation on three farms in the westernmost area of the Khomas Hochland, encroached with *A. reficiens*. The maximum tree density was found to be related to average annual rainfall and the height of the trees often being uniformly as an expression of cohorts of defined age. Under trees the nutrient

status of the soils is larger than in the open areas. The effects of the patchiness of the vegetation on soil water dynamics was not studied.

With a simple water and energy modelling approach, Caylor et al. (2005) studied the tree canopy effects on soil moisture dynamics for nine sites on a South-North Kalahari transect (one site was the Sandveld Research Station near Gobabis), where soil conditions are more or less equal, however the climate significantly changing along the transect. In the model, the soils were assumed to be a simple bucket, which means that vertical transport processes were neglected. The simulations revealed, that for the site with intermediate conditions (Sandveld shown, 405 mm a⁻¹ rainfall on average) large differences in the soil water storage under canopies compared to the inter-canopy area exist. With the definition of a soil water stress index as the frequency of the difference in stress below canopies compared to the inter-canopy space, Caylor et al. (2005) demonstrated, that savannas with intermediate precipitation amounts exhibit the largest probability of reduced water stress for trees. They explain the simulation results with reduced shortwave radiation below canopies and conclude, that the stochastic pattern of rainfall distribution effects the tree-grass-competition at the canopy patches. In dry years or drier regions sub-canopies moisture availability tends to be negatively affected by the tree whereas in moist years the sub-canopy site exhibits less water stress.

For a South African site dominated by dense stands of Mopane (*Hardwickia mopane*) Smit & Rethman (2000) studied the effect of artificial tree thinning on soil water dynamics the two seasons after the invention. They observed i) a predominantly low infiltration depth of rain water (< 0.45 m) and ii) a marked increase in evapotranspiration of the grass plot (total clearance) compared to the Mopane plots. They also present evidence, that the Mopane trees were able to utilize soil water below the commonly defined wilting point (1,5 MPa) and thus have competitive advantage to the herbaceous plants.

In Tunisia, De Boever et al.(2016) studied the role of *Acacia raddiana* trees on the near surface hydrological properties of the soil. Below tree canopies, they found more organic substance, a lower bulk density and thus higher total porosity, more macropores and higher infiltrability and in total improved soil physical conditions for water storage for the below-canopy herbaceous cover.

3 Definition of the soil water domain

By defining the compartment “soil” as a small entity of the landscape with the soil surface as the upper boundary, a defined plane in the depth of 1 m as the lower boundary and areas of about 1 m² the scheme in Figure 1 shows the involved water fluxes.

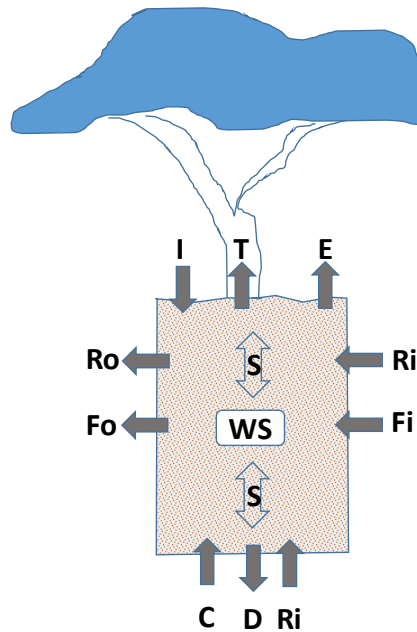


Figure 1 Scheme of water fluxes of the savanna soil compartment

Here and in accordance to Lal & Shukla (2004), the fluxes are defined as:

I = Infiltration.

The infiltration is the amount of water per timestep, which enters into the topsoil matrix through the air-soil interface. It results from precipitation (P) which is modified by interception (N), run-off (Uo) and run-on (Ui) as $I = P - N - U_o + U_i$.

E = Evaporation

Evaporation is the amount of water per timestep, which is transferred to the atmosphere directly from the bare soil surface as vapor.

T = Transpiration

Transpiration is the amount of water per timestep, which plant roots have taken up and transported within the plant to the above ground tissues and which is transferred to the atmosphere through leaves as vapor.

R = Root transport

Root transport is the amount of water per timestep, that enters (R_i) or leaves (R_o) the soil compartment through roots extending the compartment boundaries. This may be lateral roots or roots deeper as the compartment.

D = Deep percolation

Deep percolation is the amount of water, that flows out of the soil compartment below the lower boundary by gravitational forces.

F = Interflow

Interflow is the amount of water that flows in (F_i) or out (F_o) of the soil compartment through the side boundary.

C = Capillary Rise

Capillary rise is the amount of water that flows into the soil compartment through the lower boundary by capillary forces

The amount of water within the soil compartment is indicated as WS = water storage. Within the regarded timesteps there are internal water flows possible, in the scheme indicates as S = seepage.

The full equation for this soil system is given as:

$$\Delta WS = I - E - T + (R_i - R_o) + (F_i - F_o) + C - D$$

* Fluxes are in and out of the soil compartment

4 Characteristics of the study area

4.1 LOCALITY AND LAND USE

The study area is located about 110 km north of Windhoek/Namibia in the thornbush savannah of central Namibia. All plots are on a commercial rangeland farm of 13,200 ha size with about 500 – 600 cattle grazing permanently on the farm.

The topography of the area is almost flat; the altitude about 1,500 m above sea level (a.s.l.). The inselberg 'Ombutozu' with an altitude of 1,916 m a.s.l. is located at the western farm border. A net of ephemeral river systems (called riviers in Afrikaans) of the Omatako catchment drain the farm to the northeast. In the rainy season the run-off water is retained in dams and swales along the rivers.

The climate is characterized by summer rainfalls (predominantly between November and April) with mean annual precipitation of ~ 346 mm (Haarmeyer et al. 2010) and a range between 100 and 600 mm a⁻¹ (own investigations). Typical are intense rain events often combined with thunderstorms. The mean annual temperature is 20 °C, and the monthly mean air temperature range from 13 °C (in June) to 25 °C (in December). The potential evaporation rate of 1800 to 2000 mm a⁻¹ causes a strong climatic water deficit of 1500 to 1700 mm a⁻¹ (Mendelsohn et al. 2009).

Geologically, the farm is situated in an area of a bundle of rock formations, which are dominated by granites of the Damara - Granite – Intrusion (MET 2000). Other bedrocks are conglomerates of the Waterberg – Basin and schists and dolomites of the Damara – Supergroup (Winterstein, 2003). Except for the inselberg, the bedrock is almost entirely covered by a layer of loose or cemented soil material. At the investigation sites, the upper part of the bedrock is strongly weathered and the saprolite is covered with ≥ 1 m of soil material.

The study area is part of the thornbush savannah being characterised by open grass patches with scattered trees (e.g. Acacias). Furthermore, dense tree or shrub cohorts that mainly consist of bush encroachers like *Acacia mellifera* appear in the landscape.

In between these vegetation patterns mixtures with any kind of composition of grasses, herbs, shrubs and trees occur in this region. In Haarmeyer et al. (2010) the dominant plant species which are observed 2009 at the BIOTA observatory "Otjiamongombe" on the farm area of Erichsfelde, are listed.

On the farm measurements have been conducted at five plots (Table 1, Figure 2), of which each plot consisted of two soil profiles equipped with sensors to measure volumetric soil water content and soil water tension in different depth:

- Site EC is located on a slightly elevated plateau with a low shrub density and a massive layer of cemented carbonates (calcrete) near the soil surface.

- Site EG is located in a slight depression near the farm building, where the trees have been chopped and subsequent the soil surface ploughed and planted with grasses
- Site EL is located in a levelled area with patches of old Acacia trees.
- Site ES is located in a levelled area with few medium sized Acacia trees.
- Site EP is located in a pan filled with clayey sediments from the Ombutozu (dark area west of the farm boundary in Figure 2) and a medium density of medium sized Acacia trees.

The sites EC and EP have been dismantled in May 2011, as on both sites the measurement of the soil water dynamics was challenging. On EC the massive calcrete had to be opened for the installation of sensors below with the likely consequence of preferential infiltration at this position. On EP the high clay contents resulted in inaccurate soil moisture readings. Instead, in May 2011 the site EG was installed to monitor the soil water dynamics on a de-bushed area.

Table 1 Overview of the studied plots

Position	Coordinates	Soil type	Vegetation characteristics	Management	Period of measurements
EC	S -21.599 ° E 16.901 °	Petric Calcisol	dwarf shrub & grasses dominated, few bushes	Extensive grazing	9/2007 - 5/2011
EG	S -21.612 ° E 16.903 °	Chromic Luvisol	annual grasses & herbs, planted bluebuffelgrass (<i>Cenchrus ciliaris</i>)	De-bushed & ploughed (2009), intensive grazing	5/2011 - ongoing
EL	S -21.654 ° E 16.886 °	Chromic Luvisol	patches of large Acacias with dwarf shrubs & grasses in the intercanopy	Extensive grazing	9/2007 - ongoing
EP	S -21.638 ° E 16.868 °	Sodic Vertisol	Mixture of herbs & grasses, many patches of shrubs	Extensive grazing	12/2007 – 5/2011
ES	S -21.611 ° E 16.870 °	Chromic Luvisol	Dominated by grasses, scattered small trees & shrubs	Extensive grazing	9/2007 – ongoing

Due to the restricted database, the soil water dynamics of site EC and EP are not further regarded in the result chapter.

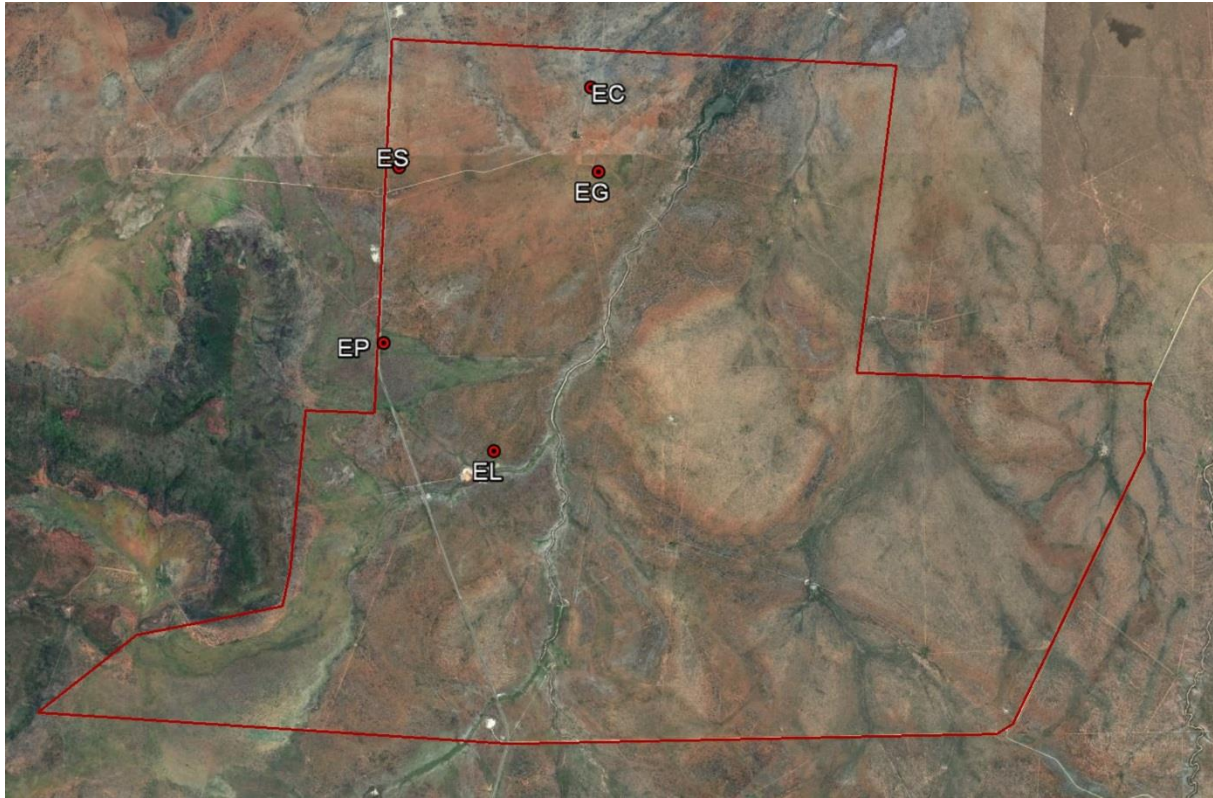


Figure 2 Location of the monitoring sites and farm boundary

4.2 SOIL PROPERTIES

According to Mendelsohn et al. (2009), the soilscape of the study area is characterized by the dominance of Chromic Cambisols. Detailed mappings resulted in a huge spectrum of other soil units (Classen 2005, Petersen 2008) such as Calcisols on calcrete dominated plateaus, Vertisols in pans and depressions and Arenosols alongside the dry riverbeds. Additionally, clay illuviation has led to a predominance of Luvisols over Cambisols within the reddish plateau areas.

At all positions, topsoil consist of sandy loam, sandy clay loam or even clay (Table 2). For the chromic Luvisols, there is a significant increase in clay content with depth of about 10 -12 %. Despite of the proportion of fine-grained particles, the soils additionally exhibit a significant share of coarse particles (medium to coarse sand).

Table 2 *Properties of soil horizons: texture*

site	ho-ri-zon no	upper boundary	lower boundary	color moist	Tex-ture	Clay	Silt	fine Sand	me-dium + coarse Sand	Sand
		m	m	Munsell		% DW	% DW	% DW	% DW	% DW
EC	1	0,00	0,10	10YR 3/3	SL	7,5	17,7	52,3	22,4	74,8
	2	0,10	0,27	calcrete						
	3	0,27	0,60	10YR 5/4	SL	17,6	17,1	46,4	19,0	65,4
	4	0,60	0,90	10YR 7/3	SCL	25,0	17,4	38,6	19,0	57,6
	5	0,90	1,10	10YR 7/3	SCL	16,2	19,3	38,6	26,1	64,7
	6	1,10	1,30	10YR 5/5	SL	6,8	49,7	25,9	17,6	43,5
EG	1	0,10	0,35	5YR 3/4	SCL	25,4	8,9	22,4	43,3	65,7
	2	0,35	0,60	5YR 3/4	SCL	33,3	9,7	22,4	34,7	57,0
	3	0,60	0,80	5YR 3/4	SCL	33,8	11,1	21,5	33,6	55,1
	4	0,80	1,70	5YR 3/4	SCL	37,2	12,1	22,1	28,6	50,7
EL	1	0,00	0,10	5YR 3/4	SL	10,2	10,1	29,7	50,0	79,6
	2	0,10	0,35	5YR 3/4	SL	15,5	8,4	29,0	47,1	76,1
	3	0,35	0,60	2,5YR 2,5/3	SL	19,2	8,9	24,5	47,4	71,9
	4	0,60	0,80	2,5YR 2,5/3	SCL	20,2	9,3	23,4	47,2	70,5
EP	1	0,00	0,14	10YR 3/3	C	47,2	22,5	14,0	16,3	30,3
	2	0,14	0,40	7,5YR 2,5/3	C	52,0	19,8	12,3	15,9	28,2
	3	0,40	0,70	10YR 3/3	C	53,1	11,8	12,1	23,0	35,2
	4	0,70	1,00	7,5YR 4/3	C	48,8	18,8	12,0	20,4	32,4
ES	1	0,00	0,10	5YR 3/4	SL	13,5	7,0	20,4	59,1	79,5
	2	0,10	0,40	5YR 3/4	SL	15,6	9,2	20,3	54,8	75,1
	3	0,40	0,70	5YR 2,5/4	SCL	20,6	10,0	22,1	47,3	69,4
	4	0,70	0,85	2,5YR 2,5/4	SCL	21,8	10,6	20,9	46,7	67,6
	5	0,85	1,00	5YR 3/4	SCL	23,9	13,1	20,3	42,8	63,0

The Vertisol exhibits the lowest bulk density due to high amount of swelling clays (Table 3). For the chromic Luvisols, bulk density in the topmost layer is larger than in the deeper layers, indicating the effect of trampling and rain drop splashing on soil properties. The soils have a high air capacity and a normal capacity to store water in plant available tension.

Table 3 *Properties of soil horizons: bulk density and porosity*

site	horizon no	Bulk density	Total porosity	Residual WC	WC at pF 2.5	WC at pF 1.8	Air capacity	Available field capacity
		g cm ⁻³	% vol	% vol	% vol	% vol	% vol	% vol
EG	1	1,440	44,94	9,76	17,12	26,58	18,36	16,82
	2	1,450	44,20	12,27	18,95	28,54	15,66	16,27
	3	1,450	45,00	13,85	20,75	28,75	16,25	14,90
EL	1	1,568	42,62	6,41	12,11	24,08	18,54	17,68
	2	1,476	47,31	7,26	11,87	21,57	25,74	14,31
	3	1,502	45,95	11,10	16,16	25,35	20,60	14,25
	4	1,511	45,35	12,80	16,01	24,62	20,74	11,82
EP	1	1,147	58,74	29,95	36,99	45,13	13,60	15,18
	2	1,182	58,05	34,44	42,27	49,21	8,84	14,77
	3	1,396	58,51	36,71	44,92	49,16	9,36	12,45
ES	1	1,488	44,86	6,01	11,37	19,93	24,93	13,92
	2	1,447	47,05	7,84	12,56	22,70	24,35	14,87
	3	1,392	49,20	9,27	15,78	25,37	23,82	16,10
	4	1,468	46,74	8,80	13,33	19,44	27,30	10,64

Except for the Calcisol at site EC and the Vertisol at EP, all profiles are slightly acid and have low amounts of soil organic carbon enriched in the topsoil (0.34 – 0.37 %, Table 4). The sum of exchangeable bases is related to the clay content.

Table 4 Properties of soil horizons: pH, EC, SOC, NT and CEC

site	hori- zon no	pH	pH	EC	SOC	SIC	NT	Su B
		in H ₂ O	in CaCl ₂	μS cm ⁻¹	% DW	% DW	% DW	mmoleq kg ⁻¹ DW
EC	1	8,0	7,1	60	1,33	2,21	0,143	248,4
	2	calcrete						
	3	8,2	7,5	76	1,30	5,34	0,079	269,2
	4	8,5	7,7	62	0,55	7,35	0,040	245,8
	5	8,6	7,8	63	0,47	6,88	0,027	246,6
	6	8,6	7,8	72	0,19	5,30	0,020	275,5
EG	1	5,6	5,2	118	0,34	0,00	0,044	
	2	6,0	5,7	158	0,31	0,00	0,048	
	3	6,1	5,4	172	0,27	0,00	0,046	
	4	6,2	5,9	131	0,21	0,00	0,042	
EL	1	6,2	5,5	22	0,35	0,00	0,045	42,1
	2	6,3	5,5	15	0,31	0,00	0,041	59,6
	3	6,3	5,5	14	0,29	0,00	0,043	77,1
	4	6,5	6,0	11	0,26	0,00	0,042	88,5
EP	1	8,7	7,7	53	0,52	0,13	0,059	361,8
	2	8,4	7,8	68	0,45	0,12	0,048	487,0
	3	8,9	7,8	74	0,41	0,14	0,048	535,4
	4	9,0	7,9	150	0,38	0,17	0,044	494,4
ES	1	6,2	5,1	20	0,37	0,00	0,045	27,3
	2	6,1	5,1	15	0,25	0,00	0,036	38,3
	3	6,3	5,4	11	0,26	0,00	0,040	50,9
	4	6,2	5,5	15	0,24	0,00	0,039	53,8
	5	6,2	5,5	11	0,27	0,00	0,045	62,4

4.3 VEGETATION

Plant analysis on 1000 m² plots at the monitoring sites ES and EL , carried out in 1998 by D. Wesuls, revealed a dominance of grasses (*Stipagrostis uniplumis*) for site ES and a coverage with shrubs and trees of 3 %. For site EL, the shrub & tree coverage was estimated with 22 %. Here, *Acacia mellifera* is the plant species with the highest coverage and in the intercanopy the dwarf shrub *Monechma genistifolium* dominates the grasses.

Table 5 *Results of plant analysis of 1000 m² plots in 1998: Dominant species and coverage*

Site ES	% cover	
Stipagrostis uniplumis	50	perennial Grass
Lycium oxycarpum	2	perennial Shrub
Acacia mellifera	1	perennial Shrub/Tree
Geigeria ornativa	1	annual Herb
Site EL	% cover	
Acacia mellifera	15	perennial Shrub/Tree
Monechma genistifolium	5	perennial Dwarfshrub
Acacia tortilis	5	perennial Tree
Stipagrostis uniplumis	3	perennial Grass
Lycium oxycarpum	2	perennial Shrub
Eragrostis jeffreysii	1	perennial Grass

More recently, the density of woody vegetation was quantified by analysis of high-resolution imagery as offered by GoogleEarth (picture from February 2010). The distribution of trees and larger shrubs have been identified by dark colour and a rim of shade in the NW direction. Through manual digitalization of these patches and using the polygon area offered by the programme, the proportion of woody vegetation has been quantified (Table 6)

Table 6 *Density of woody vegetation within 1 ha (state 2/2010)*

Position	Date of picture	Number of woody vegetation patches	Proportion of woody vegetation (%) within 1 ha
EC	12.10.2009	15	1,51
EG	1.2.2010	3	0,56
EL	1.2.2010	55	11,97
EP	1.2.2010	74	19,16
ES	1.2.2010	32	4,39



Figure 3 *Monitoring site EG (22.3.2013)*



Figure 4 *Monitoring site EL(12.3.2011)*



Figure 5 **Monitoring site ES (12.3.2011)**

5 Methods and data overview

5.1 LABORATORY METHODS

The disturbed and undisturbed samples have been analysed in the laboratory with standard methods:

- pH in CaCl₂ acc. to REEUWIJK, L. P. VAN (ED.) (2002);
- total organic carbon with an elemental analyser (vario MAX, Elementar Analysensysteme);
- bulk density with the core method (Blake & Hartge 1986);
- pore size distribution with the pressure plate technique (Soil moisture Inc. Equipment Klute 1986);
- particle size distribution acc. to DIN ISO 11277.

5.2 COMPONENTS OF SOIL WATER MONITORING STATIONS

5.2.1 Climate

At each plot, a rain gauge was installed, logging precipitation with an accuracy of 0.2 mm and in a resolution of 30 min using a tipping bucket (MCS 162, MC Systems, South Africa).

Since October 2010 a weather station according to World Meteorological Organization standards is running at 1.4 – 6.3 km from the sites (coordinates: -21.5986 °S, 16.9012 °E; data online see <http://www.sasscalweathernet.org>). In the years 2007 – 2009, a BIOTA weather station in 21 km northwest of the farm provided additional climate data (data <http://www.biota-af-rica.org>).

5.2.2 Soil water content and soil temperature

Soil water content for each profile was monitored using TDR sensors (easytest type FP/mts, Institute of Agrophysics, Poland) with 100 mm rod length, installed horizontally from an open pit in the depth 20, 40, 60 and 80 cm below soil surface, respectively and which were coupled to a logger (type TDR/MUX/mts). For the sensors, the region of influence is given by the manufacturer as a cylinder having approximated diameter of 5 cm and height of 11 cm, circumference around the sensor rods (100 mm length). Power supply was guaranteed by a 12V 6 Ah battery bloc; the daily measuring interval was fixed at 8:00, 16:00 and 24:00 hours. The sensors additionally recorded the soil temperature.

5.2.3 Soil water potential

Soil water potential is monitored with granular matrix sensors (type WATERMARK® 200SS, Irrrometer Company Inc., USA) of 22 mm diameter and 83 mm length. The sensors consist of

stainless steel electrodes imbedded in a defined and consistent internal granular matrix material. This matrix is encased in a hydrophilic material that establishes a good hydraulic conductivity with the surrounding soil and is held in place by a durable stainless steel perforated shell with plastic end caps. Four granular matrix sensors were installed in the same depth as the TDR sensors and connected to a Watermark Monitor Logger 900 M. The logging interval was set on 2 h. Sensors of both profiles were combined in one logger, which were placed in a plastic box and fixed to a rigid iron pole. In the logger the predefined soil temperature was fixed to 30 °C. The logger output was an uncorrected soil matrix potential in cbar.

5.3 DATA OVERVIEW, PROCESSING AND ANALYSIS

In general, data readout, change of batteries and control of the soil water monitoring stations took place two times per year. An exception was in 2009, when after the readout in 05/2009 the next visit of the farm was conducted in 5/2010.

5.3.1 Data overview

Soil moisture (volumetric water content, and soil water potential) were monitored from September 2007 until October 2016. However, in this period stations have been started at different moments, have been stopped and re-build and the logging devices had a number of malfunctions of different reasons. Thus, the amount of existing data varied between the stations and type of sensors. In Table 7 an overview of the existing data is given, a long version with the listing of the data gaps can be found in the appendix.

Table 7 Overview of existing raw data

Station	Start	End	Days installed	Missing days	Days data
1 Rain gauges					
EC	14.06.2007	13.03.2011	1369	402	967
EG	12.04.2011	running	2031	0	2031
EL	24.09.2007	running	3327	565	2762
EP	14.06.2007	10.04.2009	667	0	667
ES	14.06.2007	running	3429	198	3231
SASSCAL	26.11.2010	running	2168	81	2087
2 Soil water content and temperature					
EC	13.03.2008	12.03.2011	1095	583	512
EG	12.04.2011	running	2031	326	1705
EL	28.09.2007	running	3323	797	2526
EP	07.04.2008	12.04.2011	1101	581	520
ES	28.09.2007	running	3323	680	2643

Station	Start	End	Days installed	Missing days	Days data
3 Soil water potential					
EC	15.12.2007	12.03.2011	1184	371	813
EG	14.05.2011	running	1999	0	1999
EL profiles	15.12.2007	running	3245	221	3024
EL transect	15.12.2007	running	3245	636	2609
EP	05.04.2008	23.10.2008	202	0	202
ES profiles	15.12.2007	running	3245	859	2386
ES transect	15.12.2007	running	3245	782	2463

5.3.2 Mean precipitation

On the farm, rain gauges at six positions have been running for different periods (see Table 7). For every rain gauge, daily readings have been summarized and for all gauges, for which the data were reliable, daily sums been averaged as areal mean precipitation (mP). The daily means were summarized for hydrological years, that were defined as running from October 1st to September 30th.

5.3.3 Temperature corrections of soil water potentials

The soil matrix potential readings were corrected for soil temperature influences using the non-linear equation of Shock et al. (1998):

$$SMP = \frac{4,093 + 3,213k\Omega}{1 - 0,009733k\Omega - 0,01205T_s}$$

(SMP = soil matrix potential [kPa]; kΩ = resistance (kOhm); Ts = soil temperature (°C)).

As not for all data corresponding in-situ soil temperatures were available, missing values were generated using the following procedures:

- I. The measured temperature at 80 cm depth of each profile followed the seasonal trend of air temperature. Thus for each halve year a cubic regression has been calculated which was applied to the phases with missing data to the same depth.
- II. All soil temperatures in 20 cm depth were strongly correlated between each other and followed air temperature. To calculate missing values we applied linear regressions to nearest station with existing soil temperature readings or – for the phase between 10/2009 and 5/2010 where no data from own stations or locally weather station were available – from linear regressions to air temperature at the climate station in Otjiwarongo.
- III. Missing temperatures in 40 cm and 60 cm depth were linearly interpolated between 20 and 80 cm depth.

5.3.4 Balancing available soil water contents

To calculate the total soil water storage (SWC), the readings of the soil water contents (% volume) of each depth (WS_i) were multiplied with the respective depth increment of the soil layer (dm) and summed up for the profile (Table 8). The delineation between the depth increments was placed in the center between the sensor depth, thus the increment of the upper and lower sensors were larger than the middle ones.

Table 8 Depth factors for balancing total soil water storage

Sensor	Depth installation (cm)	Depth increment for calculation (dm)
1	20	3
2	40	2
3	60	2
4	80	3

5.3.5 Balancing flows to calculate deep percolation

Trying to quantify deep percolation (D) for individual phase with moist subsoil a water balance approach was applied, that was based on the flow scheme of Figure 1 and the following general equation:

$$N - I_c - \delta U = ET_a - \delta SWC + D$$

Here, the fluxes are named as N = precipitation, I_c = interception, δU = difference of runoff and runoff, ET_a = actual evapotranspiration, δSWC = change in soil water content, D = deep percolation; all fluxes given in mm.

In general, the water balance equation consist of six relevant fluxes, of which just two (N , δSWC) are monitored in high temporal resolution and the additional variable soil water potential (SWP) gives information i) when D is physically possible and ii) how much is the actual evapotranspiration (ET_a) reduced compared to the potential ET (ET_p).

All monitoring data were analysed in 8-hour timesteps (0 – 8 – 16 – 24 h per day), as the SWC-data were existing with this resolution.

Based on the following assumptions, however, an estimate of the unknown fluxes was possible:

- The **interception** (I_c) is assumed to depend on the type of vegetation and the duration of rainfall within the timestep, which was recorded in 15- minutes resolution. Per rainfall reading, I_c was calculated with 0.1 mm/reading for vegetation consisting of grasses and dwarf shrubs and 0.2 mm/reading for the canopy-areas.

- The amount of **runoff or runoff** (δU) per timestep was calculated, assuming, that during a rain event, which means typically within 8 hours or within the next two timesteps, the increase in soil water content (δSWC) has to equal infiltration.

$$\delta U \approx \delta \text{SWC} - (N - I_c)$$

This means, that we assumed, that the rain impulse did not lead to deep percolation within the timestep of the rain event itself and that E_{ta} is irrelevant within this short term.

- The **actual evapotranspiration** (E_{ta}) is known to depend on the climate conditions, the soil water availability and the type and state of the vegetation. In a first step, we calculated the potential evapotranspiration (ET_p) from weather data using the Turc equation, as given in Kappas (2009):

$$ET_p = 0,0031 * C_{\text{Turc}} * (R_G + 209) * T_m / (T_m + 15)$$

$$C_{\text{Turc}} = 1 + (50 - F_m) / 70 \text{ for } F_m < 50 \% \text{ and } C_{\text{Turc}} = 1 \text{ for } F_m \geq 50 \%$$

with C_{Turc} = a factor reflecting the air humidity, R_G = daily sum of global radiation (J/cm^2), T_m = daily mean air temperature ($^{\circ}\text{C}$) and F_m = daily mean humidity (%)

Climate data were used from the SASSCAL weather station on the farm and, if data were missing, from the neighboring station on the Omatako ranch (21 km in NW direction), where climate data were existing also before 2011.

The potential evapotranspiration was transferred to actual evapotranspiration using two factors:

$$ET_a = F_v * F_s * ET_p$$

with F_v = factor for the condition of the vegetation and F_s = factor for the availability of soil moisture. Derived from own measurements of sap-flow-data (de Blécourt et al. in prep.), F_s was defined as $F_s = 1$ for $\text{SWP} < 2.6 \text{ pF}$ and $F_s = 0$ for $\text{SWP} > 3.2 \text{ pF}$ and $1 > F_s > 0$ in the range in between. In a first estimate, the factor F_v was set to 1, but, under some conditions varied between 0.15 and 1.25 to reflect the e.g. the start of the growing season ($F_v < 1$) or a rather dense vegetation after sufficient rainfall ($F_v > 1$). For phases without rainfall and without potential deep percolation, the water balance equation reduces to

$$0 = ET_a - \delta \text{SWC}$$

and the factor F_v could be calculated from the change in soil water storage.

To adapt the daily data of ET_a to the 8-hours timesteps of the water balance date, we calculated 10 % of ET_a for 0-8 hour, 65 % of ET_a for 8 – 16 hour and 25 % of ET_a for 16 – 24 hour, based on mean sap-flow readings (de Blécourt et al. in prep.).

6 Results

6.1 CLIMATE WITHIN THE STUDIED PERIOD

The climate at the study site was presented in Haarmeyer et al (2010). Here, for the period 2001 – 2009 a mean annual precipitation of 346 mm a⁻¹ and a mean annual potential evapotranspiration of 1732 mm a⁻¹ is reported.

Table 9 *Precipitation for hydrological years measured on the farm (yellow: incomplete data; mean= sum of daily means of proper data)*

Season	SASSCAL	EC	EG	ES	EL	EP	Mean precipitation
	mm a ⁻¹	mm a ⁻¹	mm a ⁻¹	mm a ⁻¹	mm a ⁻¹	mm a ⁻¹	mm a ⁻¹
2007/08		592,0		612,2	465,4	569,2	559,7
2008/09		486,2		208,2	570,6	629,8	473,7
2009/10		0,4		364,4	7,2		366,1
2010/11	653,5	578,0	111,8	754,0	760,2		746,3
2011/12	808,6		724,2	794,0	652,0		744,7
2012/13	218,1		143,0	184,0	198,0		185,8
2013/14	373,7		383,8	400,0	546,8		426,5
2014/15	233,5		223,4	275,8	288,6		270,4
2015/16	144,4		241,0		277,6		220,9
2016/17	403,9		513,6	504,6	562,6		528,7
mean							456,0

The precipitation varied extremely between the studied hydrological years (Table 9). With an spatial average of 186 mm a⁻¹ the lowest rainfall amounts were collected in the season 2012/13. In contrast, the two preceding seasons 2010/11 and 2011/12 had a mean precipitation, which was four times higher. The mean precipitation over nine seasons was 444 ± 210 mm a⁻¹.

From the farmers view, the rainfall is not evenly distributed in the landscape. The Ombutuzo, an inselberg of about 420 m height above the surrounding landscape and just west of the farm border, is observed to attract clouds and thus to initiate higher precipitation in the western camps of the farm. However, the evidence of rainfall readings for this observation is small. The mean precipitation for the four hydrological years 2011/12 to 2014/15 resulted in 421 mm a⁻¹ for station EL (near the Ombutuzo), 413 mm for ES, 408 mm for the SASSCAL weather station and 369 mm for EG.

The mean distribution of rainfall within the year is given in Figure 6. More than 5mm/5 days can be expected after November 20, however more reliable rainfalls occur not before January 10th. Highest amounts were collected at the beginning of February, with the start of May the rain season is definitely finished.

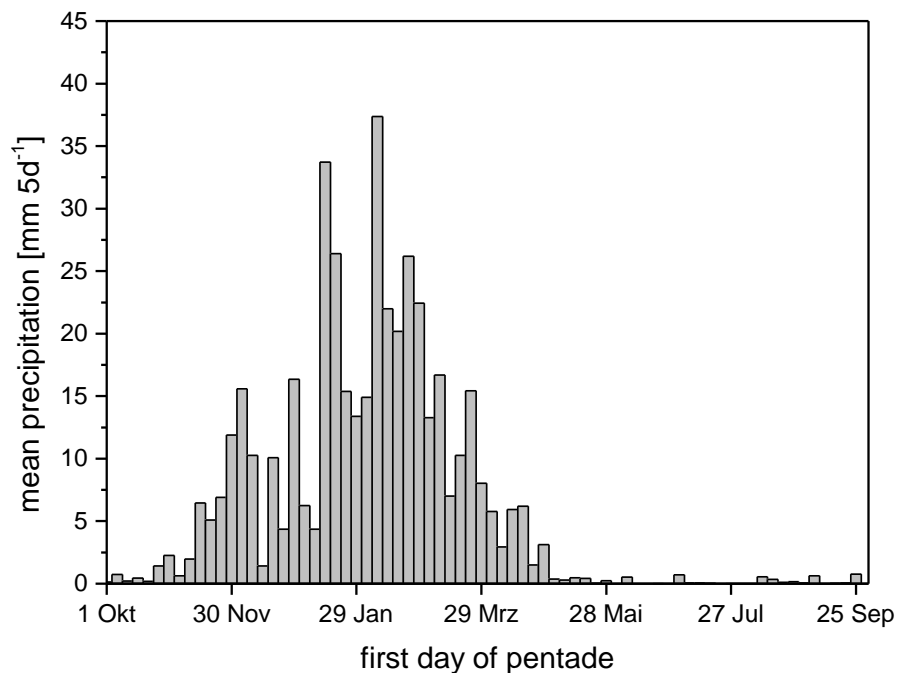


Figure 6 Mean distribution of rainfall (pentades of the season)

The most intensive rain events are listed in Table 10. Characteristically, intensive rainfall take place at thunderstorms with only local extension. These thunderstorms typically occur in the afternoon and sometimes extend in the first half of the night. For half-hour readings, the maxima have been recorded with about 40 mm, hourly readings of the SASSCAL weather station had a maximum of 56.5 mm.

Table 10 Registered most intensive rain events

Station	rank	Date	Hour	precipitation
				mm
EC	1	16.01.2009	16:00 – 16:30	26,8
	2	10.12.2008	13:00 – 13:30	19,6
	3	09.02.2009	18:00 – 18:30	17,2
EG	1	25.02.2012	13:30 – 14:00	25,6
	2	08.12.2014	09:30 – 10:00	25,6
	3	17.02.2012	16:00 – 16:30	18,4
EL	1	27.02.2009	17:00 – 17:30	39,0
	2	02.03.2009	18:30 – 19:00	36,8
	3	26.01.2011	16:30 – 17:00	34,4
EP	1	02.03.2009	18:30 – 19:00	40,4
	2	12.02.2008	23:30 – 24:00	33,4
	3	09.02.2009	18:30 – 19:00	25,8
ES	1	30.12.2010	13:30 – 14:00	31,4
	2	22.01.2012	14:30 – 15:00	29,6
	3	07.03.2008	15:30 – 16:00	28,8
SASSCAL	1	06.12.2011	01:00 – 02:00	56,5
	2	22.01.2012	15:00 – 16:00	36,8
	3	20.11.2011	16:00 – 17:00	31,1

The rainfall stations with > 2000 days of rainfall readings have been selected to calculate the inter-station correlation coefficients of daily readings (Figure 7). The correlation coefficients reduce with increasing distance, the rainfall patterns at station EL are most distinct from the other stations.

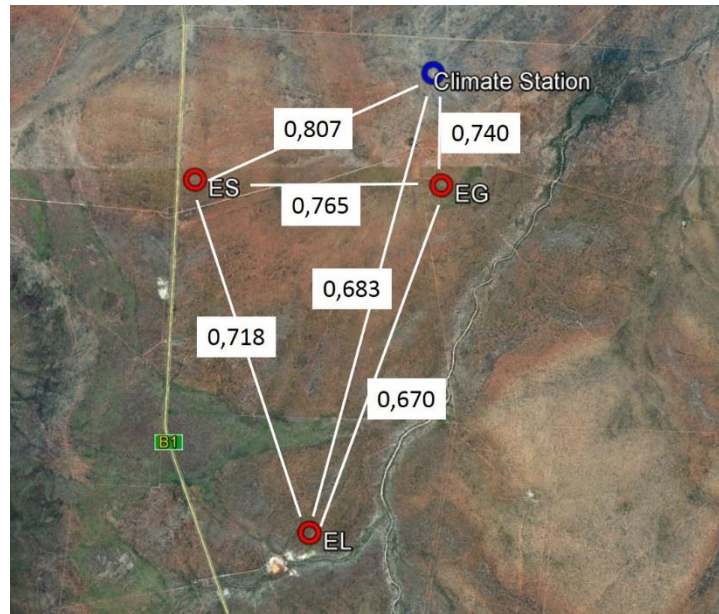


Figure 7 Linear correlation coefficients between daily rainfalls

6.2 RAINWATER INFILTRATION

The intensity of rainwater infiltration depends on climatic, vegetation and soil properties. With regard to the soil, the infiltration capacity was defined as the maximum rate of infiltration before the soil begins to pond (Lal & Shukla 2004). With the start of ponding, the precipitation has exceeded the soils capacity to infiltrate and runoff may occur. Rainfall intensities below the infiltration capacity may completely enter the soil matrix. At high rates of precipitation, the infiltration process is controlled (i) by the soil moisture, as an initially dry soil applies high suction pressure on the rainwater and thus increases the infiltration rate, (ii) by the topsoil's saturated hydraulic conductivity, which controls the infiltration rate in the wet state and (iii) by the stability of soil surface aggregates, which may break down during the rain event and clog pores in the topsoil and thus reduce infiltration. On the studied plots, the infiltration capacity varied strongly between vegetated and un-vegetated patches. The lowest infiltration rate has been observed at the un-covered patches between dwarf shrubs or perennial grass tussocks, whereas below these vegetated patches and below shrub and tree canopies higher infiltration capacities have been measured (Classen in prep.).

To analyse the effect of *Acacia mellifera* on the amount of rainwater infiltration the data have been processed with the followings steps:

- rain amounts summed for 8-hour-periods, which equals the data availability of soil water contents;
- all events with $\geq 8 \text{ mm } 8 \text{ h}^{-1}$ marked for the three stations EL, EG, ES;
- manual correction in case of two to five successive rain events of $\geq 1 \text{ mm } 8 \text{ h}^{-1}$: In these cases the rain event = sum of successive events
- initial SWC (SWC_i) defined as the SWC in 8-h-period before rain, analysed for the profile (sum of four depth intervals) and for the topsoil
- SWC after the rain (SWC_a) = maximum within 24 h including the (last) period with rain event
- increase in SWC (δSWC) calculated with $\delta \text{SWC} = \text{SWC}_a - \text{SWC}_i$

In Figure 8, for two soil profiles at site ES δSWC is shown as a result of all available rain events. The solid line represents the 1:1 relation. There is a general increase in δSWC with increasing rainfall amount (P). Linear regression between δSWC and rainfall for both, the canopy and intercanopy profile, result in:

$$\text{ES Canopy (n=56)} \quad \text{Pearson } r = 0.90 \quad \delta \text{SWC} = -4.4 + 0.8810 P$$

$$\text{ES Intercanopy (n=65)} \quad \text{Pearson } r = 0.78 \quad \delta \text{SWC} = -1.5 + 0.9157 P$$

The relation between rainfall amount and δSWC is not significantly different between the month of the season. As the correlation coefficients indicate, the association between rainfall and δSWC was stronger for the canopy position than for the intercanopy position.

In Figure 9 and Figure 10, the same relation is given, however dots marked according for three classes of SWC_i . For plot ES, the infiltration of rainwater can be characterized as:

- 1) For rain events of low intensity there is a significant likelihood that δSWC is zero or close to zero. For the canopy as well the intercanopy profile, this low intensity range is 0 ... 18 mm precipitation. For the canopy profile in 10 of 23 rain events (43 %) δSWC is $< 3 \text{ mm}$, for the intercanopy profile the probability is lower (7 of 31 rain events: 23 %).
- 2) The probability of no reaction of soil moisture depends on SWC_i (Figure 9 and Figure 10). Of all low intensity rain events ($P \leq 18 \text{ mm}$) taking place on initially dry soils ($< 30 \text{ mm}$), 33 % in the canopy profile and 27 % in the intercanopy profile show no increase in SWC. If the soil is moister, zero-reaction is much less likely.
- 3) For the canopy profile we registered one and for the intercanopy we found nine rain events, where δSWC exceeds the rain amount by a factor of ≥ 1.2 . For the intercanopy profile, these rain events are equally distributed across the months of the rain season, and have been observed at dry and at moist initial soil conditions, however not at wet.

- 4) The analysis of these events show, that initial soil moisture and the course of the rain event controls the surplus of δ SWC: If the soil is initially dry and the rainfall starts very intensive it is most likely that the increase in SWC is much higher than total rain amount. If in contrast like at the most intensive event at 30.12.10 (31.4 mm 0.5h^{-1} and 97 mm for the total event of 32.5 h), the soil has been moistened through hours of rain before, the increase in soil moisture is equal to or less than the rain amount.
- 5) In case of large rain amounts (~ 40 mm) and high initial soil water content, the deviation from the 1:1 line is most likely.

All rain events have been summarized and related to the sum of δ SWC (Table 11). For the canopy profile, about 71 % of the summarized rain could be measured as δ SWC, for the intercanopy profile this was 87 %. The mean share of rain found as increasing SWC was much less for the first rain intensity class (8 – 16 mm), here the mean δ SWC was 32 % and 58 % of rain for the canopy and the intercanopy profile, respectively.

Table 11 Rainwater infiltration at site ES – Summary of all events

(C = Canopy; IC = Intercanopy)

Precipitation class			no rain events		mean Precipitation		no * mean precipitation		mean δ SWC				no events * δ SWC	
			C	IC	C	IC	C	IC	C	IC	C	IC	C	IC
	mm	mm			mm	mm	mm	mm	mm	mm	%	%	mm	mm
1	8	16	18	24	11.59	11.59	208.66	278.21	3.68	6.71	31.7	57.9	66.2	161.1
2	16	24	13	15	19.57	19.45	254.40	291.75	13.61	16.94	69.5	87.1	176.9	254.2
3	24	32	10	10	26.40	26.40	264.00	264.00	21.62	28.71	81.9	108.8	216.2	287.1
4	32	40	8	9	36.05	36.38	288.40	327.40	28.96	33.07	80.3	90.9	231.7	297.6
5	40	48	2	2	43.20	43.20	86.40	86.40	28.55	39.70	66.1	91.9	57.1	79.4
6	48	56	3	3	52.27	52.27	156.80	156.80	45.73	55.37	87.5	105.9	137.2	166.1
7	56	64	0	0										
8	64	100	2	2	88.90	88.90	177.80	177.80	67.25	65.90	75.6	74.1	134.5	131.8
all			56	65			1436.46	1582.36			71.0	87.0	1019.8	1377.24

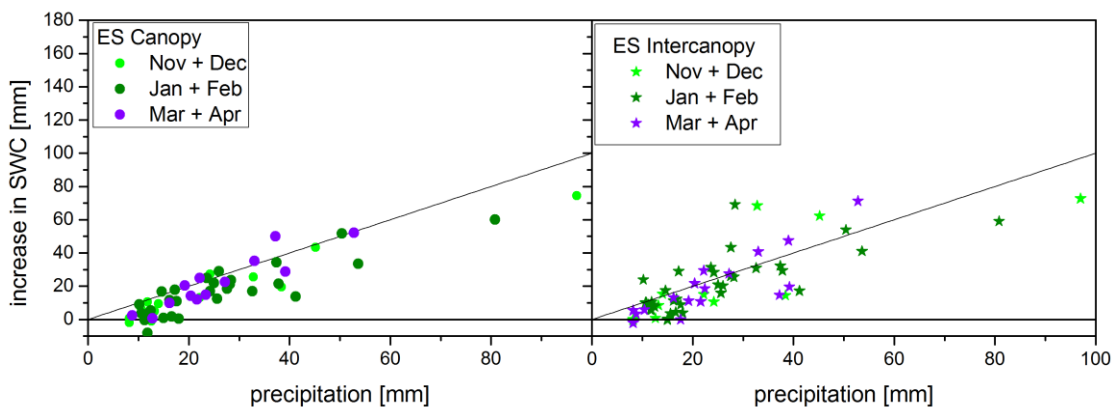


Figure 8 Increase in soil water content following rain events ($> 8 \text{ mm } 8\text{h}^{-1}$) for site ES [below canopy (left) and within intercanopy (right)] – marked month of season

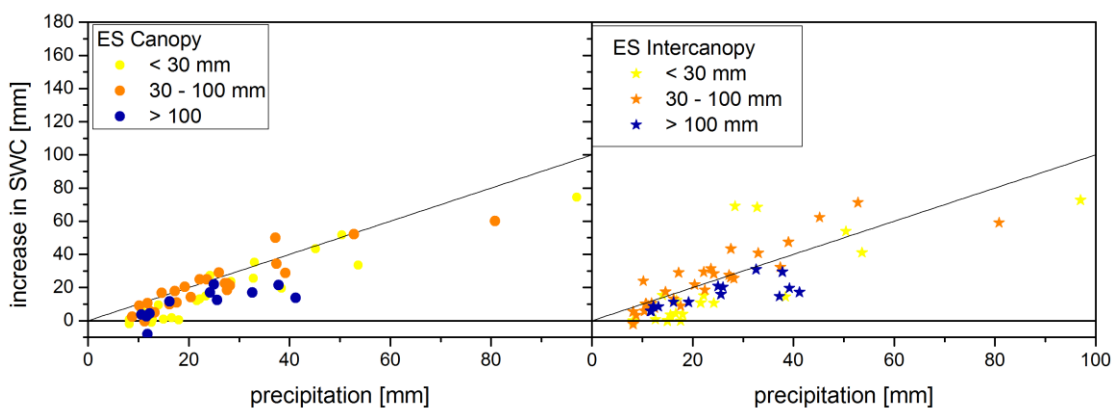


Figure 9 Increase in soil water content following rain events ($> 8 \text{ mm } 8\text{h}^{-1}$) for site ES [below canopy (left) and within intercanopy (right)] – marked initial SWC profile

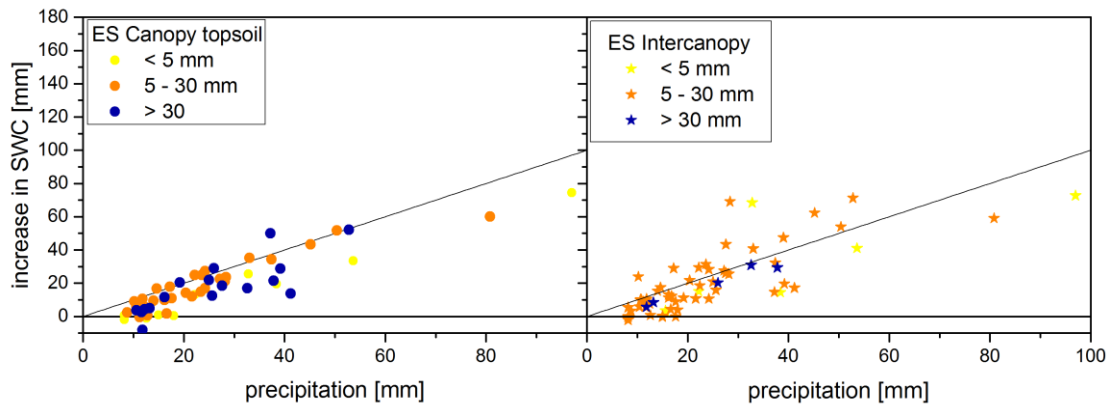


Figure 10 Increase in soil water content following rain events ($> 8 \text{ mm } 8\text{h}^{-1}$) for site ES [below canopy (left) and within intercanopy (right)] – marked initial SWC topsoil

For site EL, the respective relations are shown in Figure 11 to Figure 13. At this site where the canopy profile is located under a large *A. mellifera* patch, the reactions on the rainwater impulses are differing in part compared to site ES:

- 1) For rain events of low intensity the likelihood of zero δ SWC is large below the canopy. Here, the rainfall intensity range where zero or close to zero δ SWC is possible is expanded to $0 < P < 32 \text{ mm}$. In contrast, this range is half as large for the intercanopy site ($0 < P < 16 \text{ mm}$). For the canopy profile in 48 of 71 rain events (67 %) δ SWC is $< 3 \text{ mm}$, for the intercanopy profile the probability is much lower (4 of 57 rain events: 7 %).
- 2) As on site ES, the probability of no reaction of soil moisture depends on SWC_i . Of all low intensity rain events taking place on initially dry soils ($< 30 \text{ mm}$), 74 % in the canopy profile and 91 % in the intercanopy profile show no reaction. For the intermediate moisture class ($30 < \text{SWC} < 100 \text{ mm}$), the probability is 53 % and 47 % for the canopy and the intercanopy profile, respectively. On moist soils ($\text{SWC} > 100 \text{ mm}$), the likelihood of no reaction on rain events reduces to 13 and 34 %.
- 3) For the canopy profile we have registered seven events, where δ SWC exceeds the rain amount by a factor of ≥ 1.2 and absolutely by more than 5 mm. As can be seen in Figure 11, the increase in SWC exceeds the rainfall sometimes by a factor of up to nearly four. Of the three most intensive rainfalls at this station (see Table 10) two have led to the observed high δ SWC. Ignoring one event (23.12.2013), where δ SWC may be influenced by the event the day before, the remaining six events are characterized by the following conditions: (i) timespan between December 11 and February 27th; (ii) especially at $P > 50 \text{ mm}$; (iii) soil moisture always dry to intermediate ($\text{SWC}_i < 70 \text{ mm}$ for the profile and $< 17 \text{ mm}$ for the topsoil). The extreme events took place in December with P of about 50 mm. In contrast, the event with the highest rainfall amount (2.3.2009, $P 96.2 \text{ mm}$) resulted only to δ SWC of 19.4 mm due to high initial SWC (129 mm) and perhaps also due to a preceding rain of 12 mm in the night before.

- 4) For the intercanopy profile, there are 20 events, where $\delta \text{ SWC} > 1.2 P$ and $\delta \text{ SWC} - P > 5 \text{ mm}$. However, compared to the canopy profile, the exceedance of water infiltration is typically smaller than for the canopy profile. The events with high infiltration rates distribute in the whole rain season (November 15th – April 20th) and do occur on dry, moist and wet initial soil conditions (Figure 12, Figure 13). Nevertheless, in case of dry initial soil conditions ($\text{SWC}_i < 30 \text{ mm}$), in 43 % of analysed events the exceedance has been observed, for the moist and wet the proportion is 35 % and 9 %, respectively.

Although for the canopy profile at some events very high infiltration rates have been observed, the summary of all rain events (Table 12) shows that the total $\delta \text{ SWC}$ for this profile is 67 % of the respective rain, for the intercanopy profile, the respective proportion is 108 %. For the canopy site, especially low-intensity rains do not lead to increased soil water contents.

Table 12 Rainwater infiltration at site EL – Summary of all events

(C = Canopy; IC = Intercanopy)

Precipitation class			no rain events		mean Precipitation		no * mean precipitation		mean $\delta \text{ SWC}$				no events * $\delta \text{ SWC}$	
			C	IC	C	IC	C	IC	C	IC	C	IC	C	IC
	mm	mm			mm	mm	mm	mm	mm	mm	%	%	mm	mm
1	8	16	43	34	11.79	11.70	506.84	397.70	2.80	11.19	23.8	95.6	120.59	380.31
2	16	24	16	12	20.05	19.70	320.80	236.40	10.52	24.16	52.5	122.6	168.30	289.90
3	24	32	12	11	27.73	27.75	332.80	305.20	10.47	34.70	37.7	125.1	125.60	381.70
4	32	40	4	3	34.35	35.07	137.40	105.20	19.95	21.13	58.1	60.3	79.80	63.40
5	40	48	2	2	45.60	45.60	91.20	91.20	12.75	38.35	28.0	84.1	25.50	76.70
6	48	56	2	2	52.10	52.10	104.20	104.20	156.65	67.75	300.7	130.0	313.30	135.50
7	56	64	3	2	62.60	63.80	187.80	127.60	114.03	76.75	182.2	120.3	342.10	153.50
8	64	100	1	0	96.20		96.20		19.40		20.2		19.40	
all			83	66			1777.24	1367.50			67.2	108.3	1194.59	1481.01

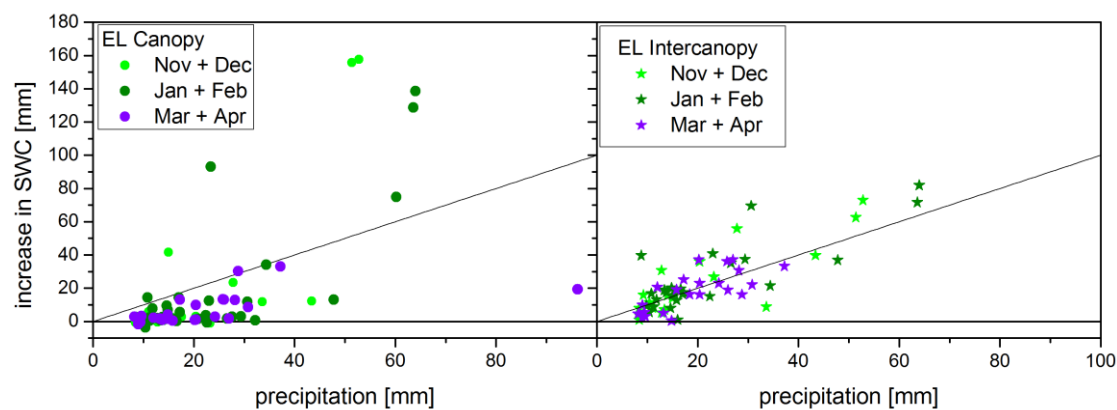


Figure 11 Increase in soil water content following rain events ($> 8 \text{ mm } 8\text{h}^{-1}$) for site EL [below canopy (left) and within intercanopy (right)] – marked month of season

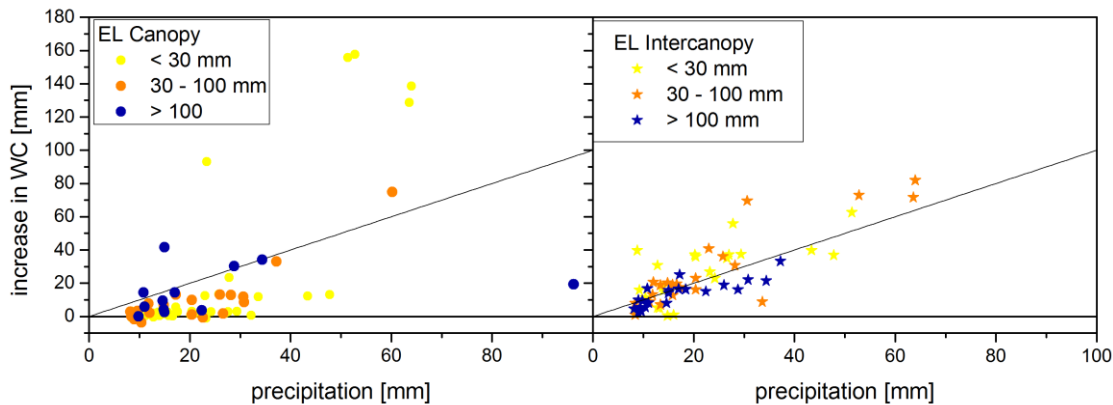


Figure 12 Increase in soil water content following rain events ($> 8 \text{ mm } 8\text{h}^{-1}$) for site EL [below canopy (left) and within intercanopy (right)] – marked initial SWC profile

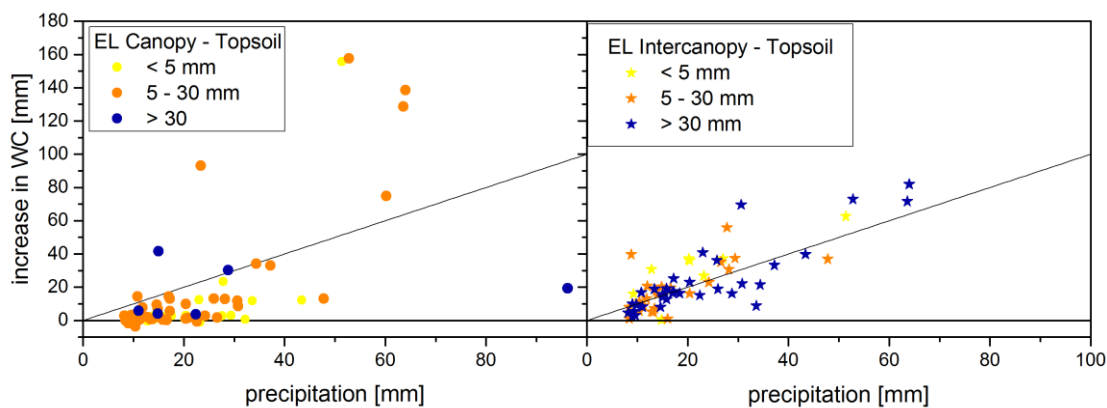


Figure 13 Increase in soil water content following rain events ($> 8 \text{ mm } 8\text{h}^{-1}$) for site EL [below canopy (left) and within intercanopy (right)] – marked initial SWC topsoil

For the cleared site EG the duration of monitoring is smaller (see Table 7). The change in δ SWC at rain events is shown in Figure 15 and Figure 16. Both profile, situated about 5 m apart and covered with grasses and herbs, differ in their reaction on rainwater inputs:

- 1) For both profiles the range of rainfall intensities with the possibility of zero δ SWC is restricted to $0 < P < 13.5 \text{ mm}$. The likelihood of zero or close to zero reaction (δ SWC is $< 3 \text{ mm}$) is 47 % for grass 1 and 59 % for grass 2 profile.
- 2) As on the other site ES, the probability of no reaction of soil moisture depends on SWC_i . Of all low intensity rain events taking place on initially dry soils ($< 30 \text{ mm}$), 40 % in the grass 1 profile and 35 % in the grass 2 profile show no reaction. For the intermediate moisture class ($30 < \text{SWC} < 100 \text{ mm}$), the probability is 21 % and 25 % for the grass 1 and the grass 2 profile, respectively. On moist soils ($\text{SWC} > 100 \text{ mm}$), the likelihood of no reaction on rain events reduces to 9 and 0 %.
- 3) For the grass 1 profile we found 22 events (62 %), where δ SWC exceeds the rain amount by a factor of ≥ 1.2 and absolutely by more than 5 mm, for the grass 2 profile,

only 5 events with these criteria have been registered. As can be seen in Figure 15, the increase in SWC exceeds the rainfall sometimes by a factor of up to ten.

- 4) The events with exceeding δ SWC do occur in all month for the profile grass 1 and are restricted to the beginning of the wet season for grass 2. There is also no preference of initial soil moisture for profile grass 1 but for grass 2 wet conditions are excluded. In dry conditions, the likelihood of extreme high infiltration rates is largest (Figure 14). With increasing SWC_i, the relation between δ SWC and rainfall decreases.

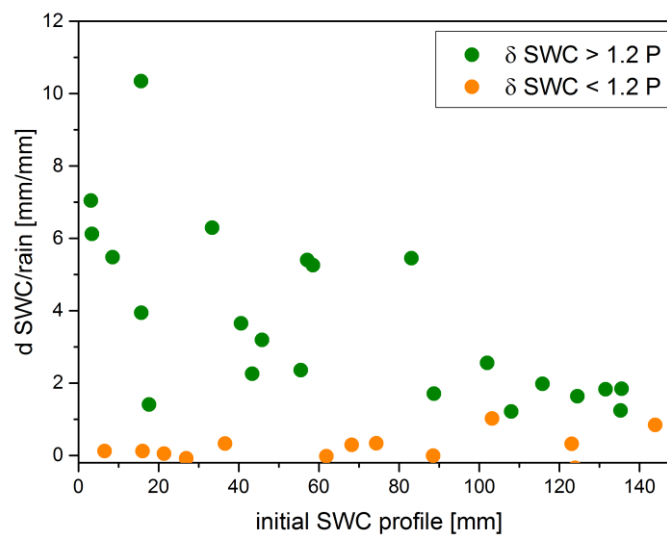


Figure 14 Relation between initial SWC and δ SWC/rain for profile grass 1 (EG)

Table 13 summarizes all registered rain event at site EG. For the profile grass 1, in total 255 % of rainfall was measured as increasing SWC. For the profile grass 2, the respective proportion was 84 %.

Table 13 Rainwater infiltration at site EG – Summary of all events

(1 = Grass 1; 2 = Grass 2)

Precipitation class			no rain events		mean Precipitation	no * mean precipitation	mean δ SWC				no events * δ SWC	
			1	2			1	2	1	2	1	2
	mm	mm			mm	mm	Mm	mm	%	%	Mm	mm
1	8	16	17	17	11,49	195,39	19,08	6,16	166,0	53,6	324,40	104,80
2	16	24	11	11	19,47	214,21	84,95	18,01	436,3	92,5	934,50	198,10
3	24	32	3	3	28,40	85,20	62,70	38,57	220,8	135,8	188,10	115,70
4	32	40	2	2	38,20	76,40	75,65	30,55	198,0	80,0	151,30	61,10
5	40	48	1	1	47,80	47,80	48,70	35,40	101,9	74,1	48,70	35,40
6	48	56	1	1	51,80	51,80	62,70	50,00	121,0	96,5	62,70	50,00
7	56	64	0	0								
8	64	100	0	0								
All			35	35		670,79			254,9	84,2	1709,70	565,10

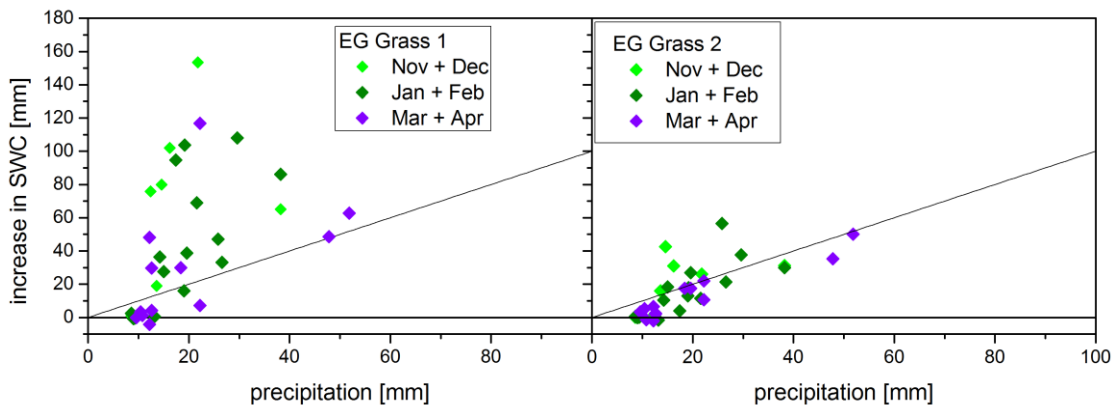


Figure 15 Increase in soil water content following rain events (> 8 mm 8h⁻¹) for site EG [grass 1 (left) and grass 2 (right)] – marked month of season

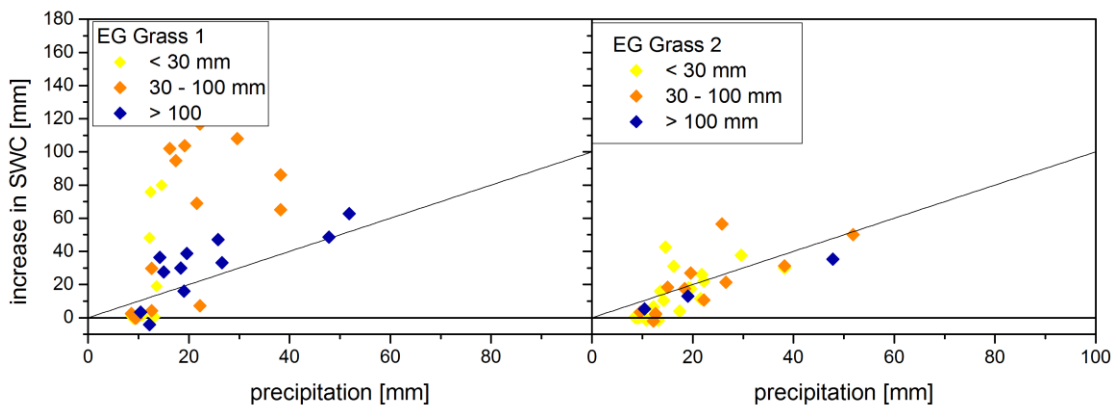


Figure 16 Increase in soil water content following rain events (> 8 mm 8h⁻¹) for site EG [grass 1(left) and grass 2 (right)] – marked initial SWC profile

6.3 EVAPOTRANSPIRATION

Once infiltrated into the soil, the water may be transferred back to the atmosphere via evaporation and transpiration. The process of evaporation depends on the topsoil moisture, the climatic situation and the soil coverage by the vegetation. In general, the amount of E is potentially high directly after the rain and reduces exponentially with ongoing desiccation of the topsoil. On the study sites, direct measurements have been carried out by Metzger (2013), Brokate (2015) and Holtorf (2016). The potential E is controlled by climatic factors, especially air temperature, the vapor pressure deficit and the wind velocity. These factors are modified by the vegetation cover, as e. g. shading reduces the ambient temperature at the soil surface and reduces wind speed and thus the exchange of moist air to upper atmosphere layers. Thus, VPD at the soil surface is reduced by the vegetation cover indirectly and so the actual evaporation.

Whereas evaporation always reduces soil moisture from the uppermost soil horizon first, via transpiration losses of soil moisture are possible in all depth intervals with living plant roots. Transpiration is coupled to the activity of plants and thus related to the density of active vegetation on a profile, which may be expressed by the leaf area index (LAI). Due to extinct wet and dry seasons in Namibian savannas and an adapted vegetation, plant activity is low to rather low from June to October and high in December to April in general. This activity pattern is, however modified by the rainfall distribution.

Within this chapter, we aim to analysis the soil moisture monitoring data with regard to the following questions:

- How much water is lost per day through the processes of evaporation and transpiration?
- Is the loss in SWC controlled by the soil water potential?
- Do the profiles vary in relation to the vegetation cover?

The following steps were applied to process the data:

- All 5-days-periods have been filtered without temporal overlap, for which the sum of rainfall of the local rain gauges was below 1 mm ($\sum P < 1$).
- From these days, those were excluded, where the subsoil water potential was above the lowest potential for rapid deep percolation in at least one day within the 5-d-period. The limit potential for rapid deep percolation was set as pF 1.8. To expand the data basis on periods, where no SWP were existing, the reference SWC for pF1.8 was calculated using the field retention curve data (details see chapter 6.4).
- The mean difference in SWC of the soil profiles between the first and last day of the 5-d-period was calculated, the sum of rainfall in the first four days of this period added, and the sum divided through the number of days (4).

$$\delta \text{ SWC} = ((\text{SWC}_{t-2} - \text{SWC}_{t+2}) + \sum P) / 4$$

- The mean SWC and the mean SWP were calculated for the 5-d-periods. Here, to compare the SWC between different profiles, for each sensor the minimum dry-season soil water content (=residual water content) was subtracted first. Thus, if SWC is given in the following chapters, this are measured values minus residual water contents.

For the canopy profile of site ES, Figure 17 shows the dependency of the daily reduction in soil water content (δ SWC) and the mean soil water content of all 5-days periods. It is obvious, that the loss in soil moisture depends on the soil water storage, the probability of higher δ SWC increases with SWC. Largest δ SWC have been registered with about 6.5 mm d^{-1} , which was found only at $\text{SWC} > 60 \text{ mm}$. Sometimes, even at high soil moisture δ SWC is low.

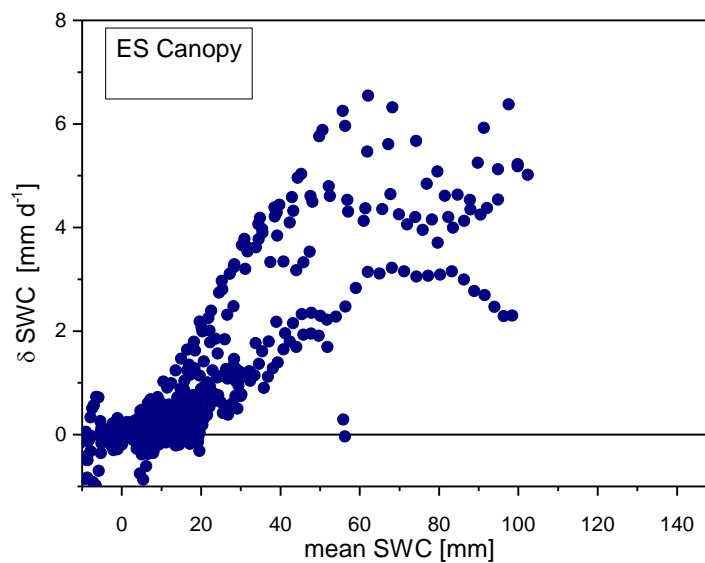


Figure 17 *Relation between SWC and loss of soil moisture (δ SWC) (both mean within four days period) for site ES – profile canopy*

The relation to soil water potential is given in Figure 18. In the canopy range, losses in soil moisture $> 1 \text{ mm d}^{-1}$ have been registered at $\text{pF} < 2.6$ with a steep increase up to the largest losses at $\text{pF} 2.1$.

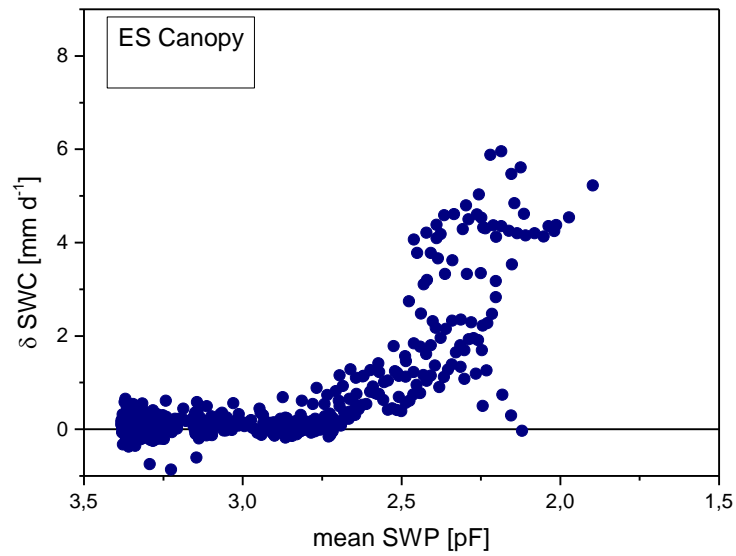


Figure 18 *Relation between SWP and loss of soil moisture (δ SWC) (both mean within four days period) for site ES – profile canopy*

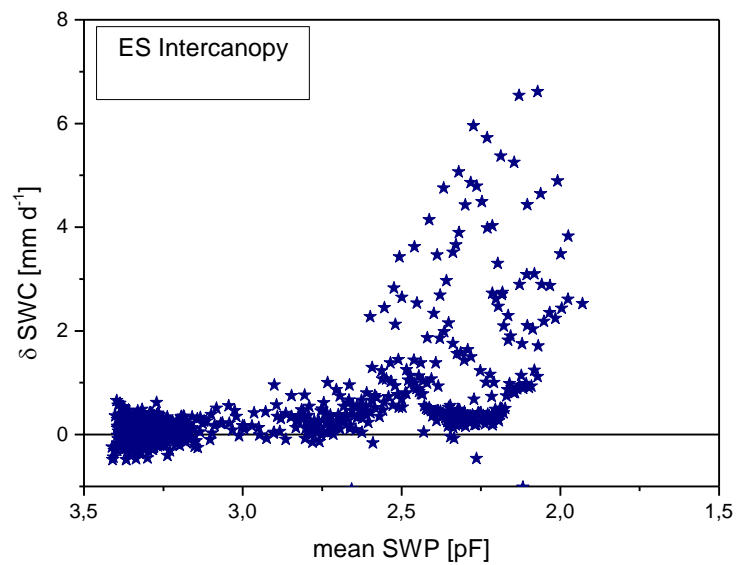


Figure 19 *Relation between SWP and loss of soil moisture (δ SWC) (both mean within four days period) for site ES – profile intercanopy*

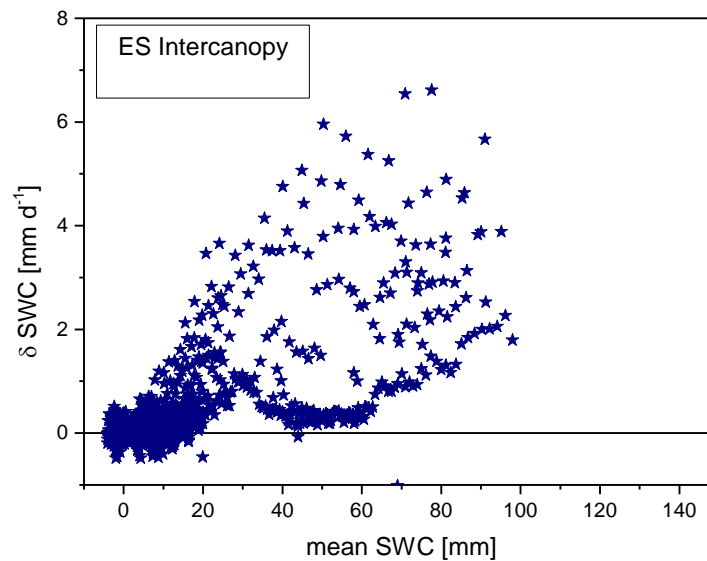


Figure 20 *Relation between SWC and loss of soil moisture (δ SWC) (both mean within four days period) for site ES – profile intercanopy*

In contrast to the canopy profile, the dry day losses in soil moisture within the intercanopy position is much more variable at the same soil moisture (Figure 21 as well as at the same soil water potential (Figure 22 **Fehler! Verweisquelle konnte nicht gefunden werden.**)). However, the general distribution with always low δ SWC at SWC < 10 mm and SWP < 2.6 pF and maxima at SWC about 60 mm and pF 2.2 has been found as well.

In Figure 21 and Figure 22, the respective graphs are given for the site EI and the canopy profile. The relation between δ SWC and mean soil moisture is comparable to the canopy profile of site ES however with a slower increase in δ SWC with increasing moisture. Here, maxima were found at SWC about > 90 mm. The total maximum was 6.8 mm d⁻¹, measured in mid of March 2009. At high soil moisture, enlarged losses in soil water contents were reliable.

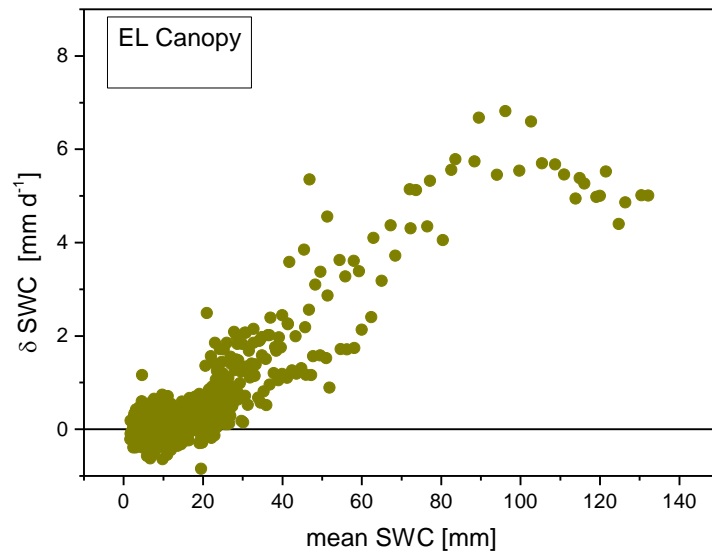


Figure 21 *Relation between SWC and loss of soil moisture (δ SWC) (both mean within four days period) for site EL – profile canopy*

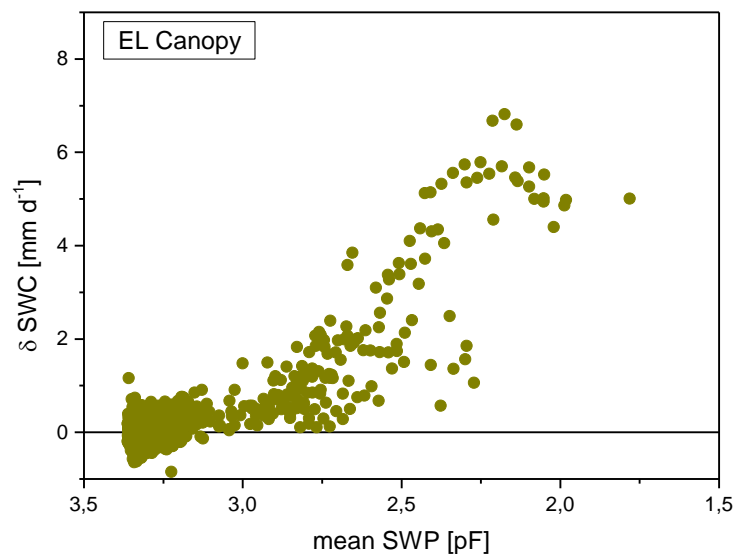


Figure 22 *Relation between SWP and loss of soil moisture (δ SWC) (both mean within four days period) for site EL – profile canopy*

Also, the relation of δ SWC to SWP is comparable at both canopy profiles. In contrast to profile ES, the canopy site at EL shows higher losses of soil moisture at intermediate soil water potentials. Here, the daily evapotranspiration may be > 1mm at a SWP < 2.9.

Within the intercanopy profile of site EL (Figure 23, Figure 24), the relation of δ SWC to soil moisture and soil water potential is extremely variable. Whereas at low SWC (< 15 mm) and

SWP ($pF > 2.8$) the evapotranspiration is always marginal, at conditions with higher moisture the losses of soil moisture is obviously controlled by additional factors. Notably low evapotranspiration rates at high moisture were observed in early days after rain events, so on 12.12.13 and 13.3.15. However, also shortly after a rain event, the highest losses in soil moisture ($\delta \text{SWC } 8.1 \text{ mm d}^{-1}$) have been found after a rain event in February 2016.

As in the canopy profiles, also for the intercanopy profiles the relation between δSWC and SWP is different between the sites in the range of $3 < pF < 2.5$.

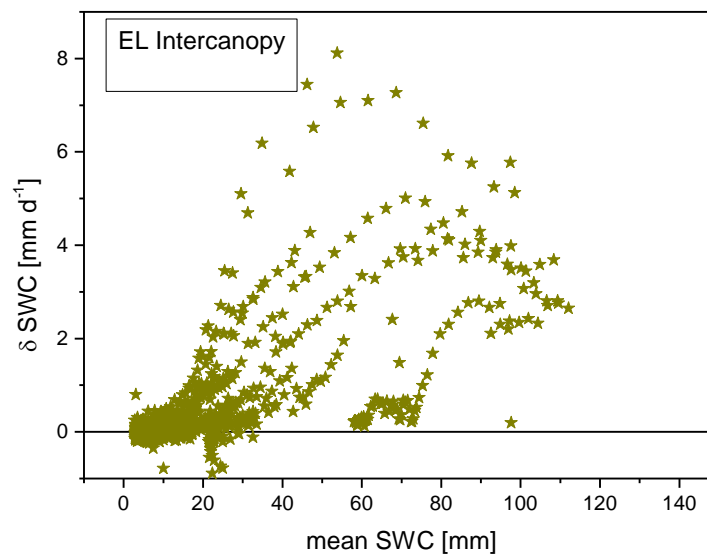


Figure 23 *Relation between SWC and loss of soil moisture (δSWC) (both mean within four days period) for site EL – profile intercanopy*

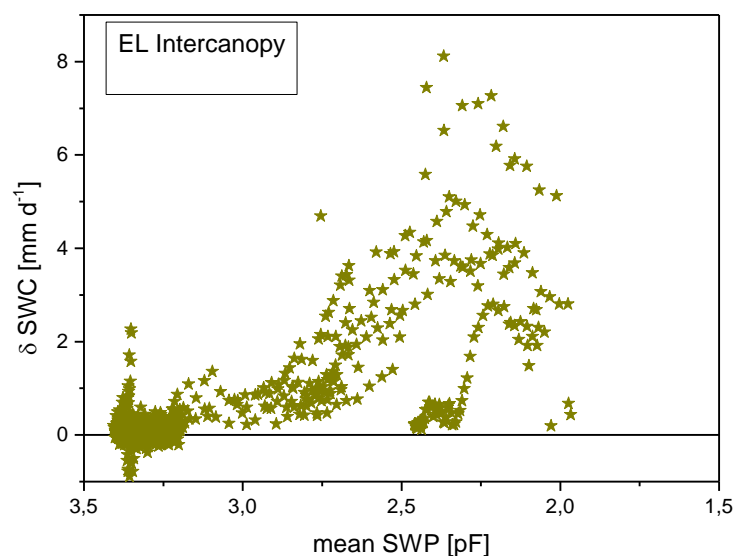


Figure 24 *Relation between SWP and loss of soil moisture (δSWC) (both mean within four days period) for site EL – profile intercanopy*

As given in Table 7, for site EG data are available only from 2011 onwards, at the beginning also with some data gaps for SWC. Thus, some moist years are not represented in the data.

The availability of soil water is significantly differing in both profiles of site EG (see chapter 6.2). However, the dry day losses in soil moisture (δ SWC) due to evapotranspiration in relation to soil moisture (Figure 26) and to soil water potential (Figure 25) are in the same range, thus for both profiles the data are presented in the same graph.

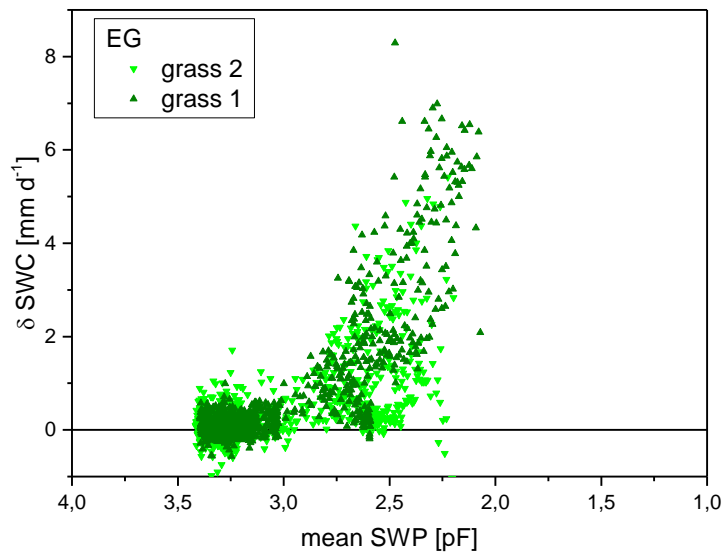


Figure 25 *Relation between SWP and loss of soil moisture (δ SWC) (both mean within four days period) for site EG – both profiles*

As in all other profile, δ SWC is low for dry profiles. For EG, potential evapotranspiration becomes larger with SWC > 15 mm and is highest (9.17 mm d⁻¹) at SWC about 87 mm and even at 60 mm above 6 mm d⁻¹). However, comparable to the intercanopy profiles, the relation between loss in soil moisture and soil water content is varying strongly and obviously controlled also by other factors.

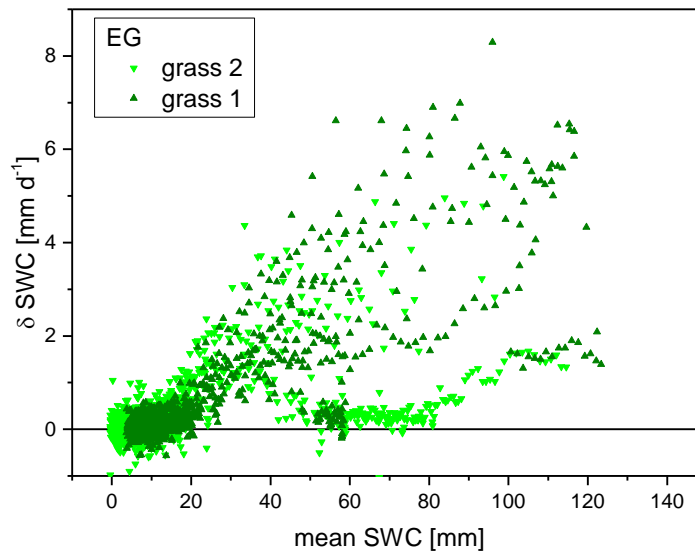


Figure 26 *Relation between SWC and loss of soil moisture (δ SWC) (both mean within four days period) for site EG –both profiles*

The relation of δ SWC to SWP indicates a very strong increase with potentials below pF 2.85. Evapotranspiration > 6 mm d⁻¹ is found at higher soil water potentials (pF < 2.4).

To compare all profiles, the relation to SWP is relevant, as in contrast to SWC this parameter is not controlled by the specific properties of the soil horizons. Thus, all relations between δ SWC and SWP were classified according to SWP and the data in all classes analysed statistically. In Figure 27 for each SWP-class the 90-percentile is presented, which can be interpreted as the dependency of the evapotranspiration potential of the studied profiles on soil moisture availability. For the classes with high moisture availability the data basis is small, thus in the range of pF < 2.2 the relation is unclear.

The graph shows, that the both profiles of site ES have irrespective of vegetation a different relation to SWP in the intermediate range ($3.0 > \text{pF} > 2.4$), however, a significant difference between the three small-scale vegetation characteristics are not significant.

In contrast, the median for each SWP-class, which represents the most likely relation between soil moisture availability and evapotranspiration, is higher for the canopy profiles than for the intercanopy positions (Figure 28) in the moist range (pF < 2.4). The both grass profiles are quite different. The profile grass 1 depicts a relation close to the canopy profile EL, whereas the profile grass 2 is more similar to the intercanopy profiles.

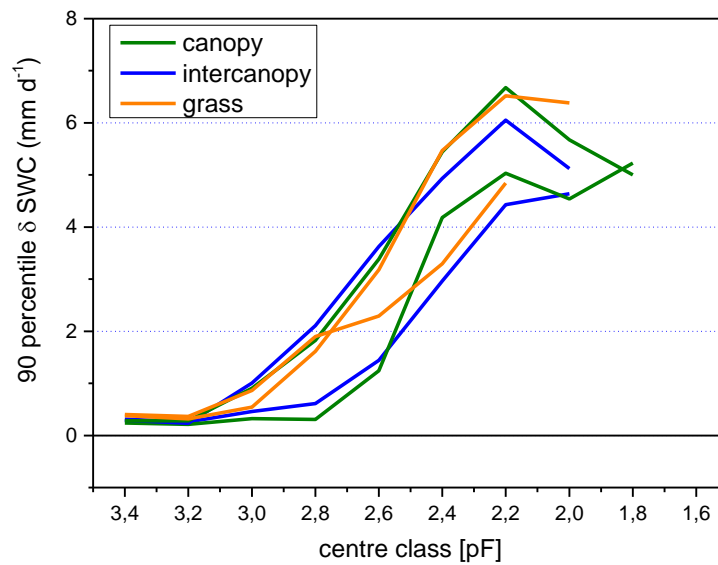


Figure 27 Upper percentile (90) of the classified relation between δ SWC to SWP for all profiles

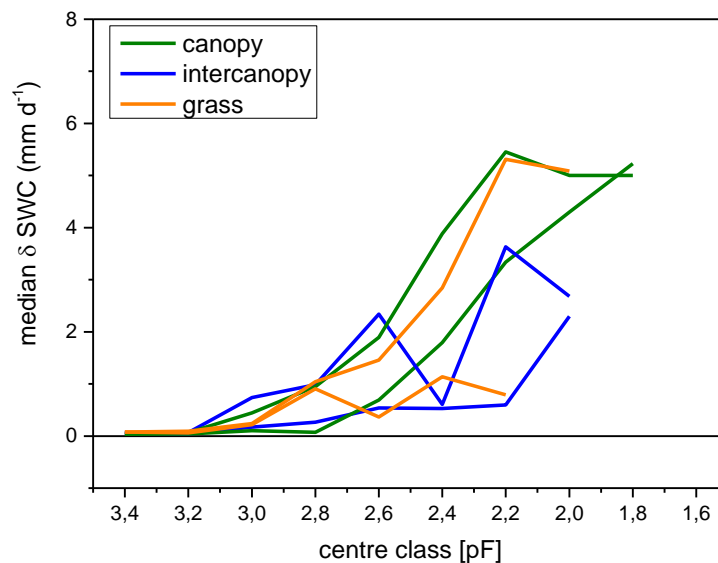


Figure 28 Median of the classified relation between δ SWC to SWP for all profiles

The total loss in soil moisture at rain-less days (δ SWC) was correlated to the measured water contents (SWC) and potentials (SWP) in different depth of the soil profiles, the results are listed in Table 14. In general highest r were found in the both canopy profiles and the profile grass 1, the lowest values in the profile grass 2. For the both intercanopy profiles the evapotranspiration is more directly correlated to the topsoil moisture, whereas in the canopy area the largest r was found in 60 or 80 cm depth.

Table 14 *Pearson correlation coefficients (r) between daily evapotranspiration and the soil water storage and availability in different soil depth (highest coefficients for each profile in bold)*

property	depth cm	ES		EL		EG	
		Intercan- opy	Canopy	Intercan- opy	Canopy	Grass 1	Grass 2
Soil water content	20	0.679	0.793	0.729	0.746	0.766	0.541
	40	0.670	0.834	0.693	0.869	0.788	0.459
	60	0.663	0.839	0.665	0.876	0.793	0.428
	80	0.661	0.676	0.622	0.882	0.772	0.403
Soil water potential	20	-0.531	-0.763	-0.731	-0.808	-0.840	-0.601
	40	-0.550	-0.765	-0.680	-0.848	-0.845	-0.545
	60	-0.534	-0.698	-0.695	-0.840	-0.801	-0.499
	80	-0.522	-0.645	-0.710	-0.847	-0.805	-0.440

6.4 DEEP PERCOLATION

As indicated in Figure 1 deep percolation (D) is the outflow of water through the lower boundary of the soil domain. Here, we defined the boundary at 1 m depth below soil surface. There is no direct measurement of deep percolation possible (see chapter 2.2), nevertheless, the existing data allow some significant implications on this flow. The deepest sensors monitoring soil water potentials (SWP) were installed in 80 cm depth. The SWP is known to be directly related to the hydraulic conductivity of the soil, as with increasing SWP larger pores of the soil become water-filled and thus the flow resistance reduces. If gradients of SWP are existing, water flow is directed from places with high SWP to those with low SWP, typically from moist to dry soil horizons (following matrix potentials) or from topsoil to subsoil (following gravitational potentials). The flow rate (Q) is described by Darcy's law, which says that Q is proportional to the hydraulic conductivity $K(\psi)$ and the potential gradient $\delta \text{SWP}/L$.

In Figure 29 measured hydraulic conductivity of few samples from site ES are presented in relation to SWP with K shown in log scale. At SWP = 2.5 pF K was found in the range of 0.01 – 0.02 mm d⁻¹, at SWP = 2.2 pF K ranged between 0.2 – 1 mm d⁻¹. Transferring these results to the subsoil means, that at higher SWP than pF 2.2 (smaller values), substantial deep percolation is possible, whereas at lower SWP deep percolation may be negligible.

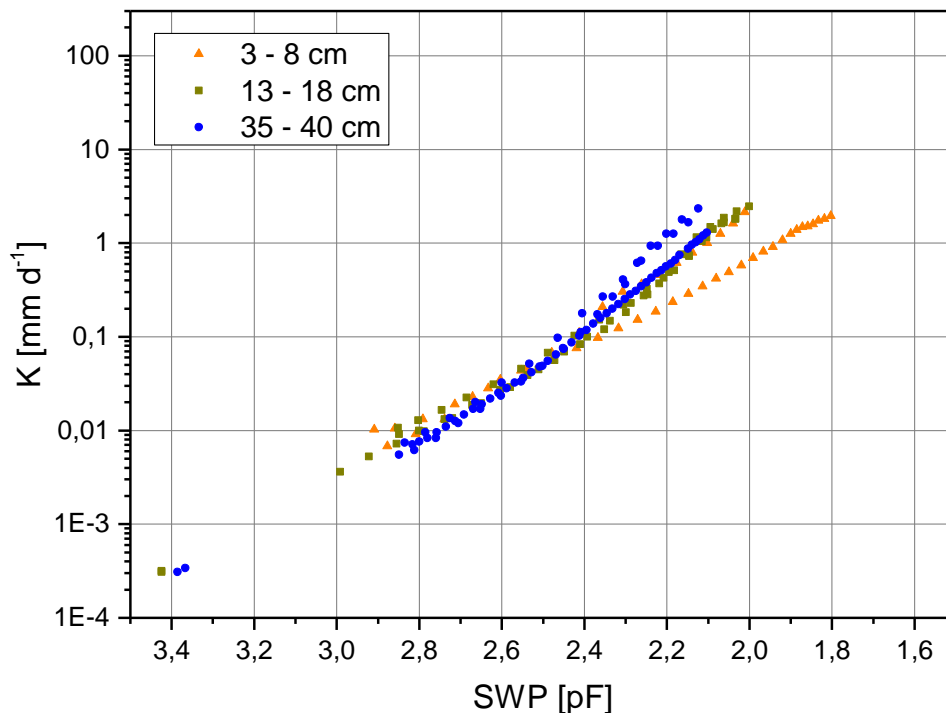


Figure 29 Measured hydraulic conductivity in relation to SWP (eight samples from site ES)

For this chapter, the available data of SWP, monitored with the granular matrix sensors, have been analysed for the subsoil. To expand the data basis to periods with missing SWP, however existing SWC, we fitted field soil water retention curves with the program RETC (Genuchten et al. 2009). The resulted values of the soil water retention curve according the model of van Genuchten (1980) allowed to calculate SWP from measured SWC. Both sets of values (daily means measured and calculated for gaps) were merged and analysed statistically.

Table 15 Frequency of moist subsoil water potentials (SWP)

Site	profile	phase	n	days with SWP ≤ 2.5 pF	days with SWP ≤ 1.8 pF	days with SWP ≤ 1.5 pF	
ES	IC	10/2007– 10/2016	3106	594	94	43	
	C		3136	342	23	0	
EL	IC		3100	521	150	102	
	C		3121	207	27	8	
ES	IC		4/2011 – 10/2016	2005	355	54	36
	C	2032		149	13	0	
EL	IC	2019		317	72	53	
	C	2032		59	0	0	
EG	Grass1	2036		416	5	0	
	Grass2	2035		259	5	3	

In Figure 30 cumulative probabilities of the SWP for the subsoil (80 cm depth) of both profiles at site ES and EL are presented. Data originate from the whole monitoring period (10/2007 – 10/2016) and thus are fairly comparable between both sites. The large proportion of dry subsoils (SWP > 3 pF, $p > 70\%$) is not shown.

For both intercanopy profiles, the probability of high SWP is significantly larger than for the canopy profiles. E.g., for the SWP class 2.0 – 2.2 pF (centre 2.1 pF), the cumulative probability for ES is $p=11.7$ and for EL $p=11.0$, whereas for the canopy profiles the probabilities are $p=6.7$ and $p=3.3$, respectively.

In Figure 31 the same type of analysis is given, however restricted to the period of 4/2011 to 10/2016. This is the period, where also data from site EG are existing and which consisted of more dry seasons. Thus, the cumulated probability of large SWP reduces compared to the data given in Figure 30, e.g. for the SWP class 2.0 – 2.2 pF (centre 2.1 pF) and the intercanopy profiles at ES $p=9.1$ and EL $p=9.2$ and for the canopy profiles at ES $p=4.5$ and EL $p=0.7$. Additionally the both profiles on site EG with grass vegetation are presented, which show a cumulated probability similar to the ES canopy profile with $p=5.6$ and $p=3.6$ for $pF = 2.1$.

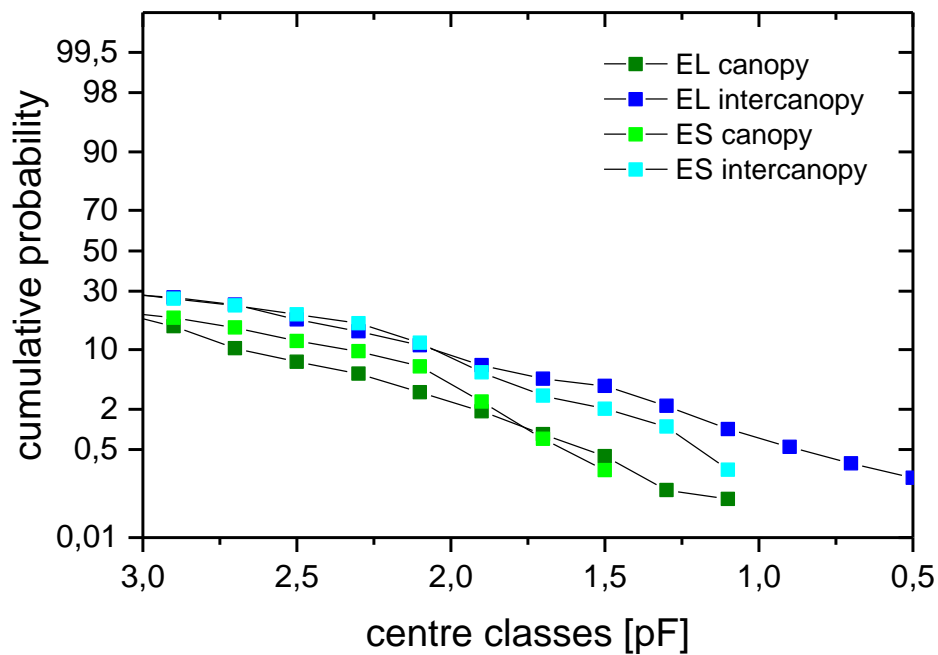


Figure 30 Cumulative probability of SWP in 80 cm depth for the phase 10/2007 – 10/2016

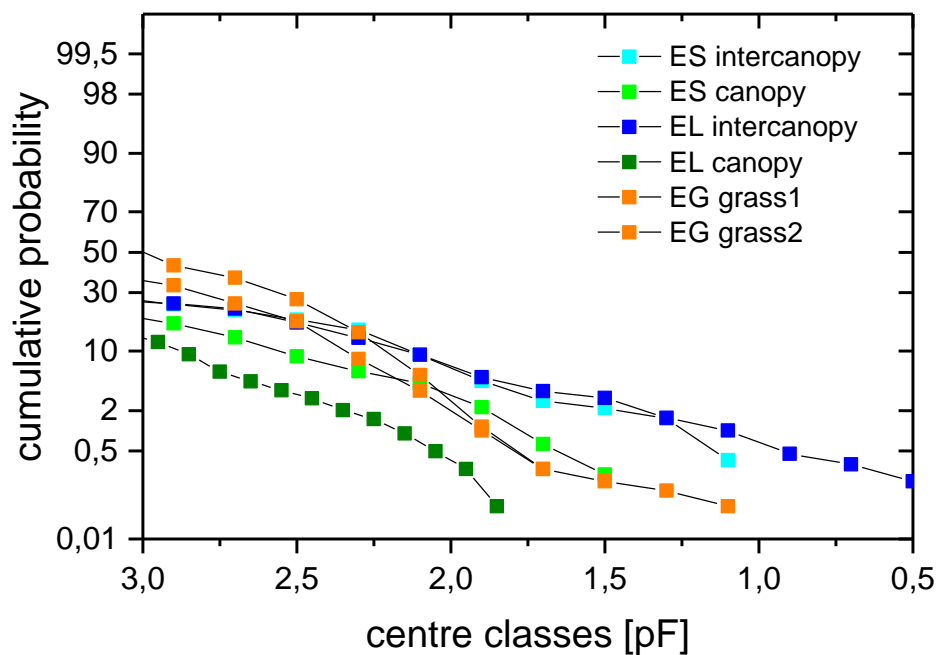


Figure 31 Cumulative probability of SWP in 80 cm depth for the phase 4/2011 – 10/2016

To compare the potential deep percolation between the profiles, the probabilities of SWP were weighed with the unsaturated hydraulic conductivity ($K(\psi)$) of the SWP class centre, as derived from Figure 29, however restricted to a maximum percolation rate of 10 mm d^{-1} . The sum of probability classes is given in Table 16. Due to the increasing $K(\psi)$ with increasing SWP,

the difference between the canopy profiles and the intercanopy profiles becomes larger. For the whole period, the probability of deep percolation in the intercanopy space is 3.17 (ES) or 3.84 (EL) higher than in the canopy space. Within the shorter period, the probability of deep percolation of both grass profiles is in the range of the ES canopy profile and significantly below both intercanopy profiles.

Table 16 *Weighed probabilities of deep percolation*

Profile	Phase 10/2007 – 10/2016	Phase 4/2011 – 10/2016
	P * K(ψ)	P * K(ψ)
	%*mm	%*mm
ES – Intercanopy	47.6	40.7
ES – canopy	15.9	15.0
EL – intercanopy	55.7	42.7
EL – canopy	14.5	2.1
EG – grass1		13.8
EG – grass2		10.1

For phases, where SWP in 80 cm depth was $pF \leq 1.8$ (moist subsoil), we calculated deep percolation using a water balance approach as explained in chapter 5.3.5. For this calculation, all data sets (SWC, SWP, weather data) were needed for each soil profile, thus, if part of the data were missing, a calculation was impossible. In total, 16 phases were identified, were at least at one of the studied profiles the subsoil had a SWP $pF \leq 1.8$. In Table 18, these phases are listed and the respective data availability given. Due to the restricted data availability, the comparison of calculated deep percolation is especially possible between the neighboring profiles and only with some limitations between the sites.

Table 17 *Phases with moist subsoil and data availability for water balance approach*

Data availability: - no data; C complete data; Mp missing SWP; Ms missing SWC

no	start	end	days	data availability					
				ES- IC	ES- BC	EL- IC	EL- BC	EG- 1	EG- 2
1	11.03.2008 08:00	18.03.2008 00:00	7	Mp	Mp	C	C	-	-
2	23.02.2009 08:00	10.03.2009 00:00	15	Mp	Mp	MS	C	-	-
3	20.01.2011 08:00	23.02.2011 00:00	34	C	C	C	C	-	-
4	08.03.2011 08:00	02.04.2011 00:00	25	C	C	C	C	-	-
5	02.04.2011 08:00	13.04.2011 00:00	11	C	C	C	C	-	-

no	start	end	days	data availability					
				ES-IC	ES-BC	EL-IC	EL-BC	EG-1	EG-2
6	13.01.2012 08:00	30.01.2012 00:00	17	C	C	Ms	Ms	Ms	Ms
7	30.01.2012 08:00	16.02.2012 00:00	17	C	C	Ms	Ms	Ms	Ms
8	16.02.2012 08:00	06.03.2012 00:00	19	C	C	Ms	Ms	Ms	Ms
9	19.03.2012 08:00	04.04.2012 00:00	16	C	C	Ms	Ms	Ms	Ms
10	13.04.2012 08:00	29.04.2012 00:00	16	C	C	Ms	Ms	Ms	Ms
11	17.12.2013 08:00	02.01.2014 00:00	16	C	C	C	C	C	C
12	18.02.2014 08:00	07.03.2014 00:00	17	C	C	C	C	C	C
13	23.03.2015 08:00	08.04.2015 00:00	16	C	C	C	C	C	C
14	14.01.2016 08:00	28.01.2016 00:00	14	C	C	C	C	C	C
15	06.02.2017 08:00	01.03.2017 00:00	23	Ms	Ms	C	C	Mp	Mp
16	01.03.2017 08:00	15.03.2017 00:00	14	Ms	Ms	C	C	-	-
17	08.02.2018: 8:00	18.02.2018 00:00	10	Ms	Ms	C	C	Ms	Ms

The number of days with moist subsoils ($pF \leq 1.8$) within the analysed phases as well as the summed deep percolation are given in Table 18. The results can be summarized as:

- For site ES, 12 phases could be analysed for both profiles. Within the growing seasons 2010/11 and 2011/12 the frequency of moist subsoils where largest for both profiles (see rainfall distribution in Table 9), however the number of days with moist subsoils were larger in the intercanopy profile compared to the below-canopy profile. The amount of deep percolation varied strongly between the events and also the relation between both profiles. Highest rates of deep percolation were calculated for a 19-d-phase in mid-February 2012 with 99 mm for the intercanopy and 73 mm for the below-canopy profile. Summarizing all comparable events, the relation of deep percolation is 332 mm pro the intercanopy profile and 154 mm for the below canopy profile, which is a relation of 2.1:1.
- For site EL for the comparison between profiles data of 11 phases are existing. Here, data from the wet season 2011/12 are missing. The number of days with moist was 102 for the intercanopy and 40 for the below-canopy profile. The sum of all phases with comparable data resulted in a deep percolation of 196 mm in the interconopy and 47 mm in the below-canopy profile, which is a relation of 4.2:1.
- For the site EG, in the wet year 2011/12 no exceedance of the subsoil water potential of $pF 1.8$ could be detected, thus we assumed that deep percolation was zero. For the profile 1 with substantial runoff, for two phases in the seasons 2014/15 and 2015/16 about 50 mm of deep percolation has been calculated, the neighboring profile was without deep percolation.
- Due to differing data availabilities, a comparison between the sites EL and ES with EG is not possible, however between EL and EG seven phases with calculated deep percolation are existing at all profiles. These data indicate, that for both, the intercanopy

and the below-canopy profile, the calculated deep percolation is nearly identical: Deep percolation intercanopy ES 146 mm and EL 134 mm; deep percolation below canopies ES 28 mm and EL 32 mm.

Table 18 *Calculated deep percolation in phases with moist subsoil*

(shaded: to compare between pairs)

no	start	ES-IC		ES-BC		EL-IC		EL-BC		EG-1		EG-2	
		days	D	days	D	days	D	days	D	days	D	days	D
			mm		mm		mm		mm		mm		mm
1	11.03.2008					0	0,0	1	0,0				
2	23.02.2009					1		3	18,3				
3	20.01.2011	20	66,1	7	20,6	25	78,6	2	31,3				
4	08.03.2011	14	36,6	2	7,4	17	0,0	0	0,0				
5	02.04.2011	2	0,0	0	0,0	3	0,0	0	0,0				
6	13.01.2012	10	24,5	3	35,4	7		0		0	0,0	0	0,0
7	30.01.2012	12	41,1	2	17,7	6		0		0	0,0	1	
8	16.02.2012	13	98,8	8	73,3	16		0		0	0,0	0	0,0
9	19.03.2012	5	21,9	0	0,0	0		0		0	0,0	0	0,0
10	13.04.2012	0	0,0	0	0,0	9		0		0	0,0	0	0,0
11	17.12.2013	4	22,2	0	0,0	8	0,0	0	0,0	0	0,0	0	0,0
12	18.02.2014	4	10,8	0	0,0	15	27,7	0	0,0	0	0,0	0	0,0
13	23.03.2015	2	0,0	0	0,0	9	22,2	0	0,0	2	50,4	0	0,0
14	14.01.2016	1	10,2	0	0,0	4	5,0	0	0,0	2	55,5	0	0,0
15	06.02.2017	10		0		12	31,4	1	15,5				
16	01.03.2017	7		3		9	31,1	0	0,0				
17	08.02.2018	0	0,0	0	0,0	5		0	0,0	0	0,0	0	0,0
all (shaded)		87	332	22	154	102	196	40	47	4	106	0	0

Averaging the deep percolation of the both intercanopy and below-canopy profiles for all phases and summarizing the means results in a total deep percolation of 389 mm in the intercanopy area compared to 172 mm in der canopy area. This equals a relation of 2.27 : 1. The sums result from 7 seasons and one phase at the end of season 2007/08, for which otherwise not data were available.

In Figure 32 the relation of the mean deep percolation of both plant cover units and the rainfall per season are given. In all years, in the intercanopy area the deep percolation exceeds the percolation within the canopy area. Whereas below canopies at least 500 mm rainfall are necessary, to produce some deep percolation, for the intercanopy area this is possible even in very dry years, provided that rain events are of high intensity. Regarding the exponential increase in deep percolation with increasing rainfall it becomes obvious, that the total sums of

deep percolation as named above predominantly originate from the both wet seasons 2010/11 and 2011/12.

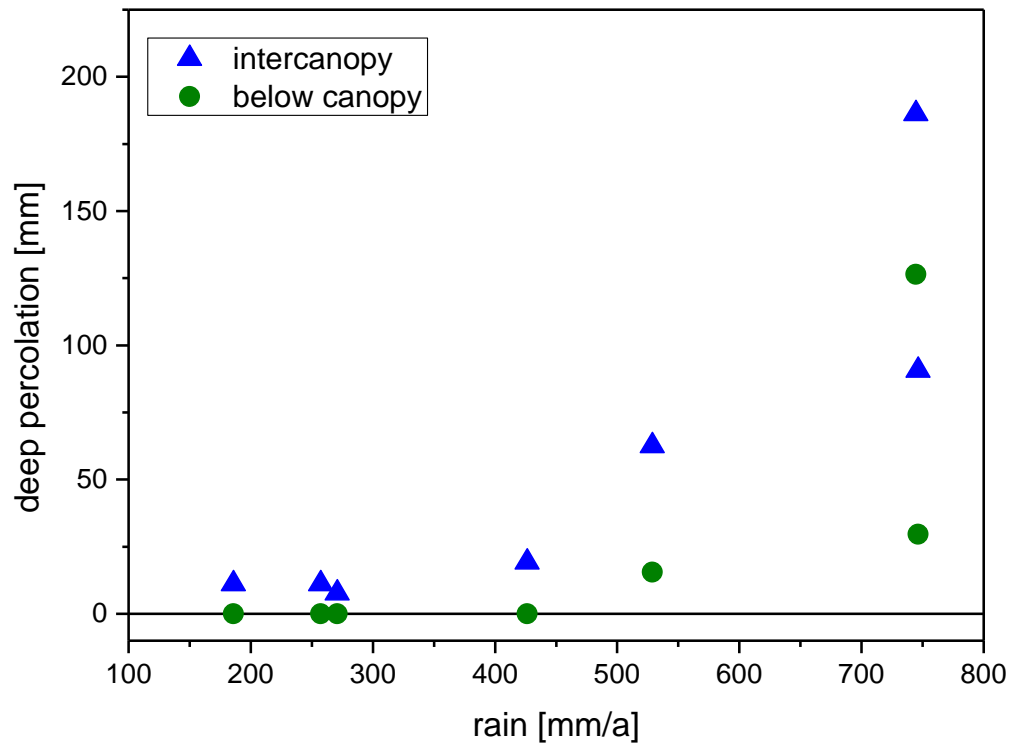


Figure 32 Seasonal deep percolation in relation to rainfall

7 Discussion and Conclusions

In this chapter, the empirical data as presented above will be discussed with regard to the questions:

1. Are the measured data reliable?
2. How do the processes interact?
3. What does this mean for the tree impact on groundwater recharge?
4. Which are the open questions?

7.1 RELIABILITY OF THE MEASURED DATA

In general, the measurement of meteorological or soil water state properties is deficient by the disturbance of the system itself, which cannot be controlled properly. Additionally, systematic errors of the sensors and logging systems as well as special features of the measuring position may result in biased data, which are difficult to interpret. To reduce the risk of data with local anomalies, the number of sensors can be enlarged.

Here, we reported measurements by three types of automatic devices:

Rain gauges

By filling a small tipping bucket, the applied rain gauges are able to register every 0.2 mm of rain within half hourly intervals. General errors of rain readings are i) the necessity to moisten the funnel of the gauge before run-off in the tipping bucket can occur (about 0.1 mm water loss for each rain event); ii) the non-registration of rain amounts < 0.2 mm and of rain amounts < 0.2 mm, which precipitate after the last tip of bucket, if in both cases sufficient time for evaporation of the water exists; iii) the potential under-catch in cases of very strong rain events, as part of the rain drains at the moment of tipping; iv) the prevention or violation of drainage into the tipping bucket due to litter and other material (e.g. bird droppings) collected in the funnel.

At all moments of data collection, the funnel have been cleaned and – if obviously clogged – respective remarks in the field book given. The principal errors of the device show, that an under-estimation of rainfall is to be expected, which may sum up to about 10 % of recorded rainfall. However, there is no way to control the amount of rainfall at events with larger precipitation.

Soil water potential (SWP) and soil water content (SWC) logging systems

The systems applied for continuously monitoring SWP is robust and simple and as given by the producer needs no calibration. As it is based on measurements of the electric conductivity in

a cylindrical porous medium of 22 cm diameter, it becomes more imprecise under low conductivity which means wet soil conditions. However, as SWP is not influenced by the surrounding matrix, the data are not affected by the local anomalies of the soil composition like rocks, biopores, cracks and others.

SWC is measured with TDR-sensors of 100 mm rod length, which are individually calibrated with dry air and pure water before installation.

For both types of soil moisture sensors, no parallel measurements with different methods to control accuracy have been performed. Nevertheless, to control the accuracy of the field data, the relation between SWP and the independent monitored soil water content (SWC) can give evidence on the reliability of both datasets. Additionally, the laboratory analysis of soil hydrological parameters can be used to check the accuracy of the field data.

Figure 33 is an example of a good relation between the both independent field measurements. It shows, that readings of SWP and SWC are strongly non-linear in a way related, which is known from many other soils and which can be fitted to typical soil water retentions curves nicely. The strong relation between both variables means, that both types of sensors are able to react on changes of soil moisture simultaneously and in an expected way.

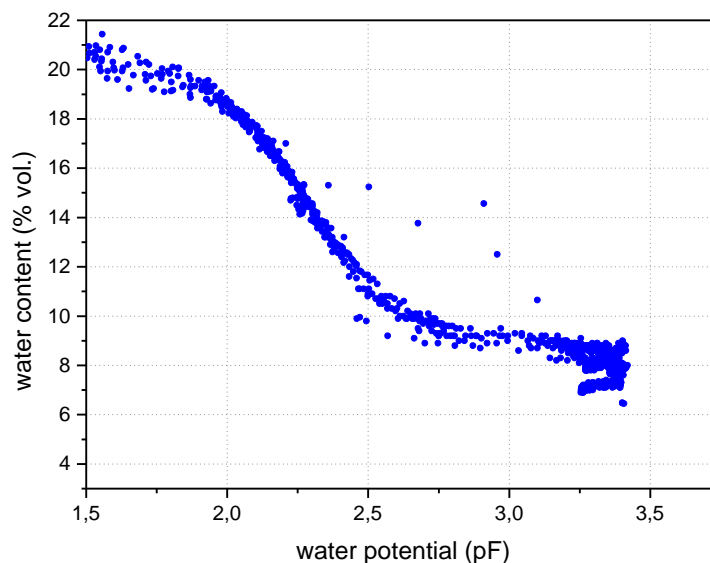


Figure 33 *Example of the relation between SWP and SWC (ES intercanopy, 80 cm) (upper limit of SWP-sensors at pF 3.3 – 3.5 in dependency of soil temperature)*

Not all positions show the relation between both sensors that perfect. However, as the sensors are not installed at the same position, differences are to be explained i) with local anomalies of the surrounding soil (for SWC) and with differing spatial patterns of soil moisture distribution.

In Table 19 two soil hydrological properties derived by different methods are compared: i) derived from laboratory analysis of soil water retention (desorption modus) and ii) derived

from the measurements of SWC and SWP in the field. For the residual water content (SWC_R), we found a linear regression of

$$SWC_{RF} = 1.0293 * SWC_{RL} - 1.149$$

(with SWC_{RF} = Dry season residual soil water content derived from field measurements; SWC_{RL} = Soil water content at pF 4.2 measured in the laboratory) with a $r^2 = 0.8198$. This means, that the dry season minimum of measured SWC can be explained with the respective laboratory values nearly perfectly with only a slight overestimation (mean error -0.87 Vol. %).

The same regression between the field capacity, here defined as the SWC at pF 1.8, resulted in the regression

$$SWC_{FF} = 0.7964 * SWC_{FL} + 2.214$$

(with SWC_{FF} = Soil water content at pF 1.8 derived from field measurements; SWC_{FL} = Soil water content at pF 1.8 measured in the laboratory) with a $r^2 = 0.3862$. Here, the prognosis of field data from the laboratory analysis is stronger varying and the mean error (-2.73 Vol %) larger.

Table 19 Comparison between soil hydrological properties measured in the laboratory and derived from field measurements of SWC and SWP

Profile	Depth	Laboratory		field measurements	
		field capacity (SWC at pF 1.8)	Residual water (SWC at pF 4.2)	field capacity (SWC at pF 1.8)	Residual water (SWC at pF 4.2)
		Vol. %	Vol. %	Vol. %	Vol. %
EG – grass 1	20		7,7	20,83	6,8
	40	26,6	9,8	23,46	9,3
	60	28,6	12,3	28,49	10,5
	80	28,8	13,9	27,01	14
EG grass 2	20		7,7	17,45	6,5
	40	26,6	9,8	21,13	9,6
	60	28,6	12,3	21,48	12,6
	80	28,8	13,9	25,18	14,3
EL inter- canopy	20	24,1	6,4	17,04	5
	40	21,6	7,3	26,34	10
	60	25,4	11,1	23,96	11
	80	24,6	12,8	27,51	12
EL canopy	20	24,1	6,4	18,31	5
	40	21,6	7,3	22,64	8,5
	60	25,4	11,1	24,59	10,5
	80	24,6	12,8	22,49	10
ES inter- canopy		19,9	6	17,46	5
	40	22,7	7,8	19,15	5,5

Profile	Depth	Laboratory		field measurements	
		field capacity (SWC at pF 1.8)	Residual water (SWC at pF 4.2)	field capacity (SWC at pF 1.8)	Residual water (SWC at pF 4.2)
		Vol. %	Vol. %	Vol. %	Vol. %
	cm				
	60	25,4	9,3	21,04	7
	80	19,4	8,8	15,88	7
ES canopy	20	19,9	6	15,16	5
	40	22,7	7,8	16,85	6
	60	25,4	9,3	19,31	7
	80	19,4	8,8	19,69	7,5

Based on both regressions, one could argue, that field data are in general a bit smaller than expected by laboratory analysis of the soils. However, the procedure in the laboratory starts with saturating the soil samples up to very high moisture followed by a step-wise dewatering up to low SWP. This practice is known to result in upper values of field observations, as in natural conditions the soil become moistened by rain and desiccated by evapotranspiration in manifold combinations, leading to characteristic hysteresis effects. Thus, the mean difference of 2.7 Vol. % for the SWC at field capacity can be explained at least in part by the hysteresis.

To summarize this topic, it seems, that both types of soil water sensors yielded in reliable data in general. The unexpected increase in water content as has been observed at different profiles and at some events thus cannot be excluded from the analysis with the argument of a malfunction of the sensors. Nevertheless, the necessity to open a pit to install the sensors and the impossibility to refill the pit in a way, which equals the original condition, opens the possibility, that soil water dynamics is altered at the pit position, which may affect the soil water dynamics at the sensor position. Most likely, this effect is stronger when i) soils water flows are influenced by preferential flows in macropores and ii) soil moisture is high.

7.2 IMPACT OF BUSH ENCROACHMENT ON THE INFILTRATION PROCESS

The analysis of the infiltration process can be summarized as:

- At all sites rain events have been observed, where the amount of local soil water increase (δ SWC) is larger, at some places much larger than measured rain amounts (P). As indicated in the discussion on the accuracy of data readings, there may be an under-estimation of rain amounts, thus only those δ SWC have been regarded as abnormal, where δ SWC is larger $P \cdot 1.2$. One explanation for this phenomenon can be the stemflow of *A. mellifera*. The funnel-shaped and smooth-barked stems and of *A. mellifera* are known to be able to collect rainwater and to transfer it to the stems base. However, the temporal distribution of the surplus of infiltration and the fact, that largest differences were found on the EG site without tree influence leads to the conclu-

sion, that this explanation is at least not dominating, perhaps not existing for the canopy profiles. The second explanation is the soil surface run-on to the measuring position at moments of rainfall. All three positions are totally flat and the topsoil composed of sandy Loam (ES, EL) or sandy Clay-Loam (EG). The aggregate stability of the topsoil is low and under splashing rainfall impact the structure tends to break down and to form a low-permeable topsoil crust. Ponding of water on the soil surface with at least short-distance flows have been observed on the farm frequently. This phenomenon explains the observed positive differences between δ SWC – P best.

- The monitoring of soil moisture started in 20 cm depth. If the topsoil was dry, it was likely, that the sensors did not react on rain events. The precipitation range with no reaction was least in the cleared site (0 – 13.5 mm), intermediate in the intercanopy profiles and the profile below a *A. mellifera* bush (ES) (0 – 18 mm) and largest in the canopy below large *A. mellifera* (0 – 32 mm).

In Figure 34, a summary of the rainwater infiltration process is indicated. Taking all measured δ SWC at rain events into account, there is a clear reduction of infiltration below large and smaller canopies. Off all rain events 29 - 33 % of rain is missing, taking the minimum amount of run-on into calculation, this proportion sums up to 29 - 55 %. The difference to rainfall results from interception, which, taking 2 mm per rain event as given by Scholes & Walker (1993) into account, may result in a deficit of about 20 % of mean rainfall. Additional processes may be stemflow not reaching the measuring position and run-off. However, the higher proportion of macropores in the topsoil below trees and the reduction of the raindrop energy through the canopy are factors, which reduce the possibility of run-off from under the canopy to nearby position.

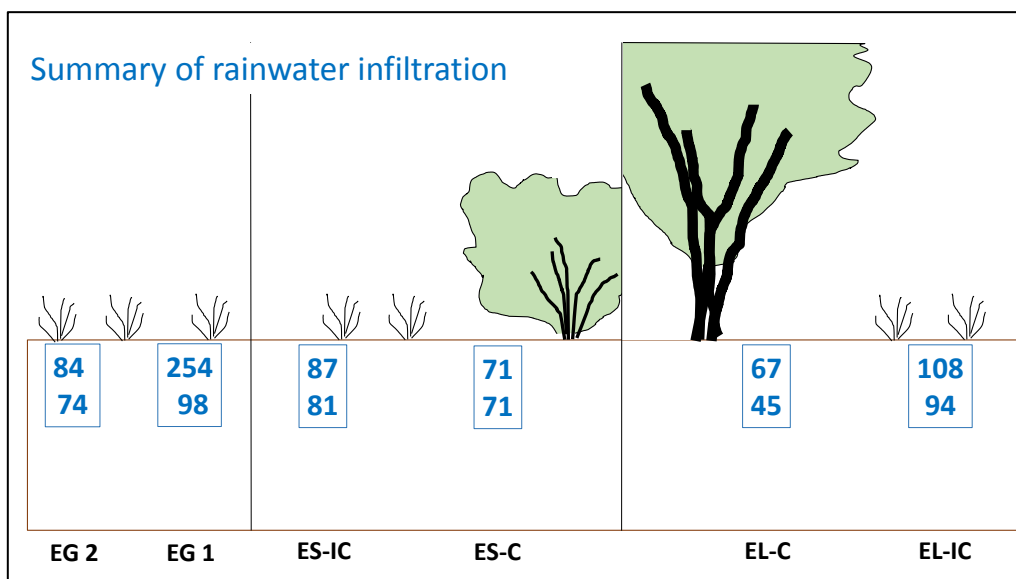


Figure 34 Summary of the proportion of rainfall infiltration (%): Upper value: all events. Lower Value: without minimum estimate of run-on

7.3 IMPACT OF BUSH ENCROACHMENT ON THE CONSUMPTION OF SOIL MOISTURE

Water vapor flows from the soil back to the atmosphere occur as evaporation from the soil surface and transpiration through root water uptake. We analysed the losses in soil water content (δ SWC) in relation to the soil water availability, the soil water potential (SWP). These losses are the sum of evaporation and transpiration, however, as losses have summed up to the depth of 1 m soil, the losses are dominated by transpiration of the plant cover.

In general, there is a strong reduction in evapotranspiration with decreasing soil water availability, at pF 3.0 for all profiles even the 90 percentile of daily δ SWC is $\leq 1 \text{ mm d}^{-1}$.

In case of moist soils ($pF < 2.3$) the different types of vegetation are able to transpire large amounts of water daily. The 90-percentile for all three types of vegetation cover (trees, incanopy dwarf shrubs & herbs, grasses) has a maximum of 6.1 to 6.7 mm d^{-1} . However, this potential is most likely only realized in case of well developed vegetation stages. For the intercanopy and one grass profile, the variation in daily water consumption at identical soil moisture conditions is large. In contrast, for the canopy profile under a large *A. mellifera* tree, the daily water uptake is strongly correlated to the soil water potential.

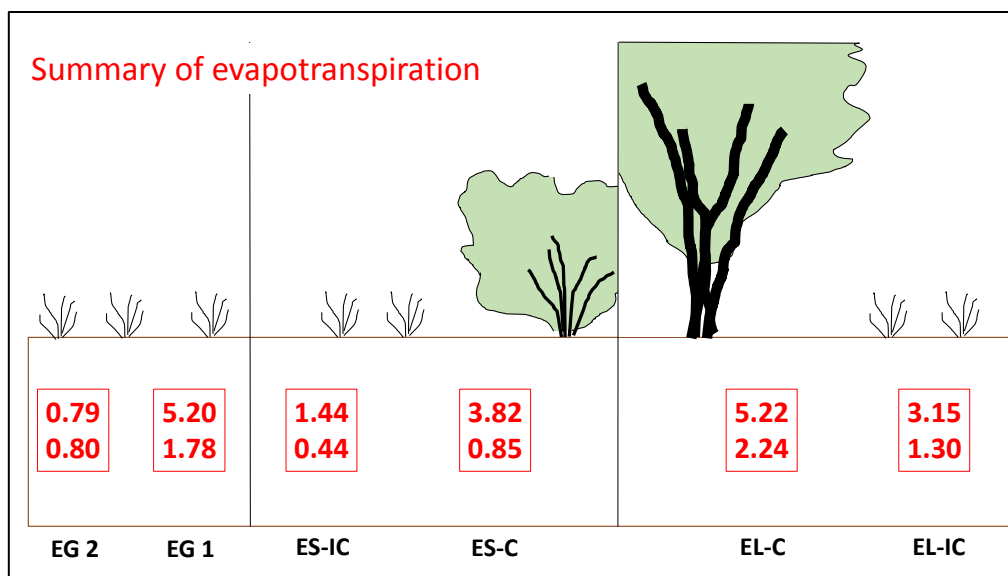


Figure 35 Summary of daily water losses by evapotranspiration ($ET, \text{mm d}^{-1}$): Upper value median ET at moist soils ($1.9 < pF < 2.3$); Lower value: median ET at intermediate soils ($2.9 < pF < 2.3$)

In Figure 35, the median ET of the different vegetation types is summarized. The small-scale comparisons of site ES and site EL clearly indicates, that soil moisture below canopies is consumed in higher daily rates than in the respective intercanopies. The ratio $ET_{\text{canopy}}/ET_{\text{intercanopy}}$ varies between 1.7 and 2.7. The absolute values of one of the both grass plots however is in the same magnitude of daily ET as has been found for the large *A. mellifera* at site EL.

The difference in daily ET between canopy and intercanopy patches is however superimposed by the variation of available soil moisture. As below canopies the rainwater infiltration is less

than in the intercanopy, part of the clear differences in ET diminish. In the consequence, the available water below canopies is transpired faster than in the intercanopy area at especially at the end of the wet season water reserves have been observed in the intercanopy space.

7.4 IMPACT OF BUSH ENCROACHMENT ON POTENTIAL DEEP PERCOLATION

As a consequence of modified infiltration and varying root water uptake between canopy and intercanopy patches, also the frequency of soil water availability in the subsoil is altered by the trees. An overview of the results of the frequency distribution weighed with the unsaturated conductivity, is shown in Figure 36. For the 9-years period (with roughly 1 year of missing data) the both intercanopy profiles exhibit a potential for deep percolation, which is 3.0 (site ES) to 3.8 (site EL) larger than the respective canopy profiles. This is the result of both, the higher infiltration and the slower evapotranspiration. The grass site, which can only be compared to the other site in the period from 2011 onwards, shows an index for potential deep percolation, which is in the range of the canopy profile of ES, but significantly larger than the canopy profile EL.

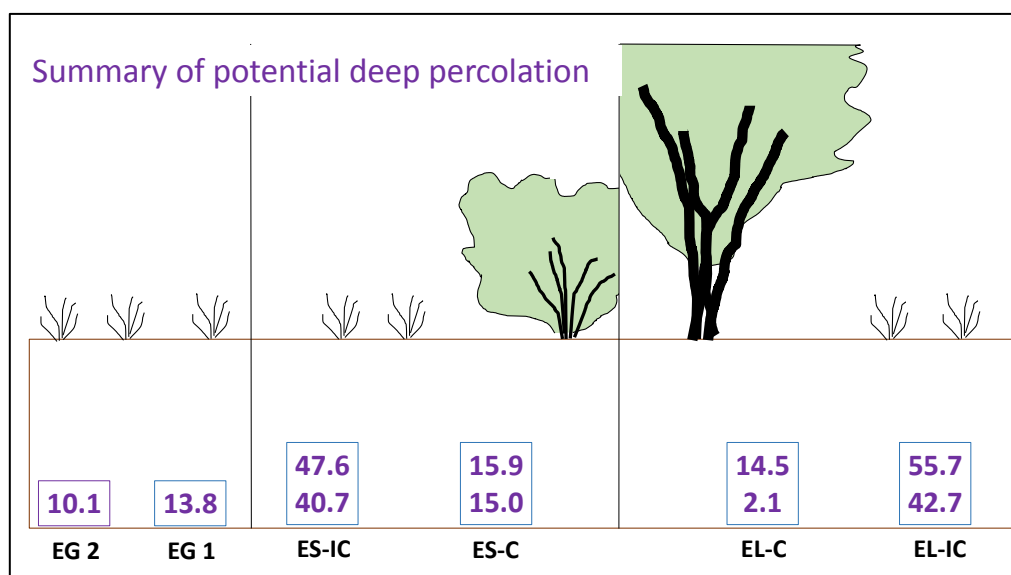


Figure 36 Summary of potential deep percolation (%* mm d⁻¹): Upper row weighed percentage for the period 10/2007 – 10/2016; Lower row for the period 4/2011 – 10/2016, respectively

At the intercanopy site EL, at some days soil water potentials near saturation have been observed ($pF < 1.0$). These values indicate a reduced potential for deep percolation at the lower boundary of the soil though the saprolite into the granitic bedrock.

Calculations of the deep percolation based on a water balance approach confirmed the findings from above and could add numbers to the amount of deep percolation. For the intercanopy site ES, where data from the wet seasons 2010/11 and 2011/12 were existing, a maximum of nearly 100 mm deep percolation has been calculated for 19 days in mid-February 2012 and a total of about 330 mm for all wet phases. Within the intercanopy, the deep percolation exceeded the amount in the below-canopy profile with a factor of 2.1 for ES and 4.2 for EL. As far as comparable, both sites ES and EL did not differ in deep percolation.

7.5 CONCLUSIONS, OPEN QUESTIONS & OUTLOOK

Based on nine years of soil water monitoring in four profiles in central Namibia, the local effects of *Acacia mellifera* on the soil water dynamics could be quantified and compared to nearby intercanopy profiles. The trees modify the infiltration and the root water uptake and thus reduce the duration of higher soil moisture in the subsoil. In comparison between two canopy profiles, of which one was below a medium sized single-standing tree, the other below a patch of large-sized old trees, the impact of the tree on the soil water dynamics was stronger below the larger tree. On the compared sites, the trees did reduce the probability for deep percolation to roughly 1/3. For phases with potential deep percolation, the calculated sums of the both below-canopy profiles were $\frac{1}{2}$ to $\frac{1}{4}$ of the respective intercanopy profiles. Additional reductions are possible, if tree roots do extract water from layers $> 1\text{m}$, e.g. from fissures out of the underlying bedrock.

A third site, for which data from five seasons were available, was located in a cleared area, thus the influence of trees on soil water dynamics could be excluded. Here, in two neighboring profiles the soil water availability as well as the soil water extraction by the grasses and herbs varied substantially between each other. For this sites, the analysed indicators of soil water dynamics differ from the intercanopy sites and were more comparable to one canopy profile. One reason may be the higher clay content and the deeper soil development at the grass site.

The influence of short-distance (?) run-off and run-on processes on soil water dynamics, as was observed on all sites and in strongest development on the clay-rich grass site, undermines the classical analysis of soil water budgets and the possibilities to model soil water fluxes, as water inputs are modified by unknown spatial and temporal variable features. However, the local variation of infiltration is likely to be a basic requisite for the deep percolation of water out of the root zone.

The study could improve the knowledge about the local effects of trees on soil water dynamics in a loamy plateau landscape of central Namibia and thus the probability of groundwater recharge. These processes on the local scale form the basis to understand hydrological processes on the landscape scale. Within the SASSCAL project in the meantime similar analysis have been started in two different landscapes, who's data basis is still too small to draw conclusions. However, also for these studies the linkage between the demonstrated water dynamics in the

soil and the groundwater level changes are still unknown and will stay unknown, as the measuring infrastructure for groundwater monitoring is not existing. The relocation of water by surface run-off and run-on and the likely influence of soil organisms like termites are factors, which enlarge the complexity of the water dynamics in these water restricted ecosystems.

Thus, to date the question regarding the effect of de-bushing on groundwater recharge cannot be answered properly. As given in the introduction, the quantification of groundwater recharge is challenging in general. For the bush-encroached drylands of Namibia a larger scale analysis of groundwater dynamics combined with studies like this, with analysis of tree species water consumption patterns with sap-flow devices and with monitoring of the vegetation dynamics are likely to solve the open question at least for some of the dominant landscape types.

8 References

- Archer, S. R. 2010.** Rangeland Conservation and Shrub Encroachment: New Perspectives on an Old Problem. *Wild rangelands: Conserving wildlife while maintaining livestock in semi-arid ecosystems*(6):53.
- Belsky, A., Amundson, R., Duxbury, J., Riha, S., Ali, A. and Mwonga, S. 1989.** The effects of trees on their physical, chemical and biological environments in a semi-arid savanna in Kenya. *Journal of applied ecology*:1005-1024.
- Bennett, S. J., Bishop, T. F. A. and Vervoort, R. W. 2013.** Using SWAP to quantify space and time related uncertainty in deep drainage model estimates: A case study from northern NSW, Australia. *Agricultural Water Management* 130:142-153.
- Blake, G. R. and Hartge, K. H. 1986.** Bulk density. Pages 363 - 375 in A. Klute, ed. *Methods of Soil Analysis: Part 1 Physical and Mineralogical Methods*, Second Edition. American Society of Agronomy, Madison.
- Briggs, J. M., Knapp, A. K., Blair, J. M., Heisler, J. L., Hoch, G. A., Lett, M. S. and McCARRON, J. K. 2005.** An ecosystem in transition: causes and consequences of the conversion of mesic grassland to shrubland. *BioScience* 55(3):243-254.
- Brokate, R. 2015.** Small scale variation in Evapotranspiration of bush encroached sites in Namibia Master of Geoscience Master University of Hamburg, Hamburg. 49 pp.
- Butler, M. and Verhagen, B. T. 2001.** Isotope studies of a thick unsaturated zone in a semi-arid area of Southern Africa. *Isotope Based Assessment of Groundwater Renewal in Water Scarce Regions*, IAEA-Tecdoc-1246:45-70.
- Caylor, K. K., Shugart, H. H. and Rodriguez-Iturbe, I. 2005.** Tree canopy effects on simulated water stress in Southern African savannas. *Ecosystems* 8(1):17-32.
- Chen, C., Eamus, D., Cleverly, J., Boulain, N., Cook, P., Zhang, L., Cheng, L. and Yu, Q. 2014.** Modelling vegetation water-use and groundwater recharge as affected by climate variability in an arid-zone Acacia savanna woodland. *Journal of Hydrology* 519, Part A:1084-1096.
- Christelis, G. and Struckmeier, W. 2001.** Groundwater in Namibia an explanation to the Hydrogeological Map. Pages 128. Ministry of Agriculture, Water and Rural Development, Windhoek.
- Christian, C. 2010.** Desk top Study on the Effect of Bush Encroachment on Groundwater Resources in Namibia. Pages 109 and Appendix. Colin Christian & Associates CC, Windhoek.
- Classen, N. 2005.** Überprüfung von Verfahren zum Up-scaling von Bodeneigenschaften in der Dornbuschsavanne Namibias Unveröff. Diplomarbeit an der Universität Hamburg, Hamburg. 111 S. pp.
- De Boever, M., Gabriels, D., Ouessar, M. and Cornelis, W. 2016.** Influence of Acacia Trees on Near-Surface Soil Hydraulic Properties in Arid Tunisia. *Land Degradation & Development* 27(8):1805-1812.
- Eldridge, D. J., Bowker, M. A., Maestre, F. T., Roger, E., Reynolds, J. F. and Whitford, W. G. 2011.** Impacts of shrub encroachment on ecosystem structure and functioning: towards a global synthesis. *Ecology Letters* 14(7):709-722.
- Genuchten, M. T. v., Simunek, J., Leij, F. J. and Sejna, M. 2009.** RETC version 6.02 Code for Quantifying the Hydraulic Functions of Unsaturated Soils. University of California, Riverside.
- Haarmeyer, D. H., Luther-Mosebach, J., Dengler, J., Schmiedel, U., Finckh, M., Berger, K., Deckert, J., Domptail, S. E., Dreber, N., Gibreel, T. and others. 2010.** The BIOTA Observatories. Klaus Hess Publishers, Göttingen & Windhoek.
- Holtorf, K.-K. 2016.** Dry season evaporation and transpiration measurements on Namibian savanna sites Master of Geoscience Master of Geoscience. University of Hamburg, Hamburg. 71 and appendix pp.

- Huxman, T. E., Wilcox, B. P., Breshears, D. D., Scott, R. L., Snyder, K. A., Small, E. E., Hultine, K., Pockman, W. T. and Jackson, R. B. 2005.** Ecohydrological Implications of Woody Plant Encroachment. *Ecology* 86:308 - 319.
- Joffre, R. and Rambal, S. 1993.** How tree cover influences the water balance of Mediterranean rangelands. *Ecology* 74(2):570-582.
- Kappas, M. 2009.** Klimatologie. Klimaforschung im 21. Jahrhundert - Herausforderung für Natur- und Sozialwissenschaften. Heidelberg: Spektrum Akademischer Verlag, 358 p.
- Kinzelbach, W., Aeschbach, W., Alberich, C., Goni, I., Beyerle, U., Brunner, P., Chiang, W., Ruedi, J. and Zoellmann, K. 2002.** A survey of methods for groundwater recharge in arid and semi-arid regions. Early warning and assessment Report series, UNEP/DEWA/RS 2(2).
- Klerk, N. d. 2004.** Bush encroachment in Namibia. Pages 253 p., Windhoek.
- Klute, A. 1986.** Water retention: laboratory methods. Pages 635-662 in A. Klute, ed. *Methods of Soil Analysis: Part 1—Physical and Mineralogical Methods*, Second edition. American Society of Agronomy, Madison.
- Lal, R. and Shukla, M. K. 2004.** Principles of soil physics. CRC Press, New York & Basel.
- McCarthy, T. and Rubidge, B. 2005.** The story of earth and life - A southern Africa perspective on a 4,6 billion-year journey. Cape Town.
- Mendelsohn, J., Jarvis, A., Roberts, C. and Robertson, T. 2009.** Atlas of Namibia: A Portrait of the Land and its People. Cape Town. South Africa: David Philip Publishers.
- Metzger, J. C. 2013.** Factors of Evaporation in Savanna Ecosystems - A Field and Model Approach Master Thesis. University of Hamburg, Hamburg. 112 pp.
- O'Connor, T. G., Puttick, J. R. and Hoffman, M. T. 2014.** Bush encroachment in southern Africa: changes and causes. *African Journal of Range & Forage Science* 31(2):67-88.
- Petersen, A. 2008.** Pedodiversity of southern African drylands PhD thesis at the University of Hamburg, Hamburg. 374 p and appendix pp.
- Reeuwijk, L. P. v. 2002.** Procedures for soil analysis, 6th Edition. International Soil Reference and Information Centre, Wageningen. 101 pp.
- Scanlon, B. R., Keese, K. E., Flint, A. L., Flint, L. E., Gaye, C. B., Edmunds, W. M. and Simmers, I. 2006.** Global synthesis of groundwater recharge in semiarid and arid regions. *HYDROLOGICAL PROCESSES* 20(15):3335-3370.
- Scholes, R. J. and Archer, S. R. 1997.** Tree-Grass interactions in Savannas. *Annual Review of Ecology and Systematics* 28:517 - 544.
- Scholes, R. J. and Walker, B. H. 1993.** An African savanna: synthesis of the Nylsvley study. Cambridge University Press, Cambridge.
- Shock, C. C., Barnum, J. M. and Seddigh, M. 1998.** Calibration of Watermark Soil Moisture Sensors for Irrigation Management. Proc. International Irrigation Show.
- Smit, G. N. and Rethman, N. F. G. 2000.** The influence of tree thinning on the soil water of a semi-arid savanna of southern Africa. *Journal of Arid Environments* 44:41 - 59.
- Van Auken, O. W. 2000.** Shrub invasions of North American semiarid grasslands. *Annual review of ecology and systematics* 31(1):197-215.
- van Genuchten, M. T. 1980.** A Closed-form Equation for Predicting the Hydraulic Conductivity of Unsaturated Soils1. *Soil Sci Soc Am J* 44(5):892-898.
- Vries, J. J. D., Selaolo, E. T. and Beekman, H. E. 2000.** Groundwater recharge in the Kalahari, with reference to paleo-hydrologic conditions. *Journal of Hydrology* 238:110 - 123.
- Walter, H. 1954.** Die Verbuschung, eine Erscheinung der subtropischen Savannengebiete, und ihre ökologischen Ursachen. *Plant Ecology* 5(1):6-10.
- Ward, D. 2005.** Do we understand the causes of bush encroachment in african savannas? *African Journal of Range and Forage Science* 22(2):101 - 105.
- Wiegand, K., Ward, D., Saltz, D. and Ezcurra, E. 2005.** Multi-scale patterns and bush encroachment in an arid savanna with a shallow soil layer. *Journal of vegetation science* 16(3):311-320.

- Wilcox, B. P. and Thurow, T. L. 2006.** Emerging issues in rangeland ecohydrology: vegetation change and the water cycle. *Rangeland Ecology & Management* 59(2):220-224.
- Winterstein, C. 2003.** Röntgendiffraktometrische Tonmineralbestimmung an Böden Namibias. Unpublished Diploma Thesis at the University of Hamburg, Hamburg. 97 p. pp.
- Zhang, L., Dawes, W. and Walker, G. 2001.** Response of mean annual evapotranspiration to vegetation changes at catchment scale. *Water resources research* 37(3):701-708.